



The University of
Nottingham

UNITED KINGDOM • CHINA • MALAYSIA

Ajigboye, Olubukola O. and Lu, Chungui and Murchie, Erik H. and Schlatter, Christian and Swart, Gina and Ray, Rumiana V. (2017) Altered gene expression by sedaxane increases PSII efficiency, photosynthesis and growth and improves tolerance to drought in wheat seedlings. *Pesticide Biochemistry and Physiology*, 137 . pp. 49-61. ISSN 1095-9939

Access from the University of Nottingham repository:

http://eprints.nottingham.ac.uk/43566/8/Accepted%20Manuscript_PBP_Ajigboye%20et%20al_2016.pdf

Copyright and reuse:

The Nottingham ePrints service makes this work by researchers of the University of Nottingham available open access under the following conditions.

This article is made available under the Creative Commons Attribution Non-commercial No Derivatives licence and may be reused according to the conditions of the licence. For more details see: <http://creativecommons.org/licenses/by-nc-nd/2.5/>

A note on versions:

The version presented here may differ from the published version or from the version of record. If you wish to cite this item you are advised to consult the publisher's version. Please see the repository url above for details on accessing the published version and note that access may require a subscription.

For more information, please contact eprints@nottingham.ac.uk

1 **Altered gene expression by sedaxane increases PSII efficiency, photosynthesis and**
2 **growth and improves tolerance to drought in wheat seedlings**

3 Olubukola O. Ajigboye^a, Chungui Lu^{a1}, Erik H. Murchie^a, Christian Schlatter^b, Gina Swart^b
4 and Rumiana V. Ray^{a*}

5 ^aSchool of Biosciences, University of Nottingham, Sutton Bonington, Loughborough,
6 Leicestershire LE12 5RD

7 ^bSyngenta Crop Protection, Schwarzwaldallee 215, 4058 Basel Switzerland

8

9 * **Corresponding author**; email Rumiana.Ray@nottingham.ac.uk

10 ¹**Present address:** School of Animal Rural & Environmental Sciences, Nottingham Trent
11 University, Brackenhurst Campus, Southwell, Nottinghamshire NG25 0QF

12

13 **KEYWORDS**

14 Sedaxane, Photosystem II, Gene expression, Drought, Wheat

15

16 **ABSTRACT**

17 Succinate dehydrogenase inhibitor (SDHI) fungicides have been shown to increase PSII
18 efficiency and photosynthesis under drought stress in the absence of disease to enhance the
19 biomass and yield of winter wheat. However, the molecular mechanism of improved
20 photosynthetic efficiency observed in SDHI-treated wheat has not been previously elucidated.

21 Here we used a combination of chlorophyll fluorescence, gas exchange and gene expression
22 analysis, to aid our understanding of the basis of the physiological responses of wheat
23 seedlings under drought conditions to sedaxane, a novel SDHI seed treatment. We show that
24 sedaxane increased the efficiency of PSII photochemistry, reduced non-photochemical
25 quenching and improved the photosynthesis and biomass in wheat correlating with systemic
26 changes in the expression of genes involved in defense, chlorophyll synthesis and cell wall
27 modification. We applied a coexpression network-based approach using differentially
28 expressed genes of leaves, roots and pregerminated seeds from our wheat array datasets to
29 identify the most important hub genes, with top ranked correlation (higher gene association

30 value and z-score) involved in cell wall expansion and strengthening, wax and pigment
31 biosynthesis and defense. The results indicate that sedaxane confers tolerant responses of
32 wheat plants grown under drought conditions by redirecting metabolites from defense/stress
33 responses towards growth and adaptive development.

34

35 1. INTRODUCTION

36 Drought is considered the most important environmental factor limiting growth, plant
37 metabolism and crop productivity worldwide [1]. Photosystem II (PSII) is the most important
38 protein-pigment complex in the chloroplast that is also most vulnerable to drought stress [2].
39 Under severe drought, often associated with elevated leaf temperatures and light levels, the
40 limitation in CO₂ uptake coupled with an increased excitation energy in PSII and absorption of
41 light energy in excess of that required for photosynthesis causes an imbalance between PSII
42 activity and the Calvin cycle. This can result in photodamage to the PSII oxygen-evolving
43 complex [3],[4], disruption of D1 protein involved in PSII repair, and subsequent inactivation
44 of PSII reaction centers [5]. To protect the chloroplast, plants have evolved photoprotective
45 responses to rapidly dissipate excess excitation energy as heat. Thermal dissipation of light
46 energy by the light-harvesting antenna complex of PSII, measured as non-photochemical
47 quenching (NPQ), is one of the most important rapidly activated regulatory mechanisms in
48 plants to avoid irreversible photodamage [6]. NPQ is triggered by the light-driven build-up of a
49 transthylakoid proton gradient (ΔpH). The acidification of the thylakoid lumen results in the
50 protonation of PSII LHC antenna regulatory proteins such as PsbS [7] and the de-epoxidation
51 of xanthophyll cycle pigment violaxanthin into zeaxanthin [6],[8]. Whilst reducing the likelihood
52 of photoinhibitory damage, NPQ momentarily reduces the quantum yield of CO₂ assimilation.
53 Although this is a highly regulated process that reduces the likelihood of oxidative stress,
54 photoprotection can also be considered to compete with photochemistry for absorbed energy
55 [9]. Plant under drought stress typically show rapid increase in NPQ with increasing
56 illumination coupled with decreased capacity for photosynthesis [10]

57 Fungicides of the class of succinate dehydrogenase complex II inhibitors (SDHIs) however
58 have been recently shown to significantly increase the efficiency of PSII photochemistry
59 (F_v/F_m') of wheat grown under drought stress, in the absence of disease, resulting in
60 improved photosynthesis and yield under controlled and field conditions [11],[12]. Changes in
61 F_v/F_m' were detected in plants grown in field and under controlled environments within 4 h of

62 fungicide application. F_v'/F_m' is indicative of changes in PSII operating efficiency attributed to
63 thermal dissipation, which correlates in a non-linear fashion with decreasing thermal
64 dissipation of excitation energy in the light harvesting complexes of PSII, estimated as non-
65 photochemical quenching or NPQ [2]. Thus it is likely that increased PSII efficiency (indicated
66 as F_v'/F_m') and improved photosynthesis in SDHIs treated plants may be accompanied by
67 reductions in NPQ. It is currently unclear how this effect on PSII and photosynthesis occurs:
68 the succinate dehydrogenase (SDH; succinate: ubiquinone oxidoreductase) complex plays a
69 central role in mitochondrial metabolism, catalyzing the oxidation of succinate to fumarate and
70 the reduction of ubiquinone to ubiquinol, thereby linking the tricarboxylic acid (TCA) cycle and
71 the electron transport system. In fungi, SDHIs specifically block the ubiquinone-binding sites
72 in the mitochondrial complex to disrupt cellular respiration and energy generation [13].
73 Although the mode of action of these compounds on fungal metabolism is well understood,
74 the effects on plant metabolism and the molecular basis of the observed physiological
75 responses to drought stress in SDHI treated plants remain unknown.

76 In this work, we investigated the effects of sedaxane, a novel SDHI fungicide, belonging to the
77 chemical class of pyrazole-carboxamides, formulated to use on crops as seed treatment to
78 provide local and systemic protection of the seed, seedling and roots against soil-borne plant
79 pathogenic fungi [14]. The active ingredient is typically absorbed from the soil matrix by the
80 developing plant roots and translocated within the seedling with systemic activity of 4-6 weeks
81 following seed germination. We combined chlorophyll fluorescence with gas exchange
82 measurements to measure PSII efficiency and photosynthesis of plants grown from sedaxane
83 treated seeds. Our aim was to better understand the molecular mechanism for improved
84 photosynthetic efficiency, growth and biomass of SDHI-treated wheat grown under drought
85 stress in the absence of disease using transcriptomics approach. The objective of this paper
86 was to address the following questions. (1) Can sedaxane improve photosynthesis and PSII
87 efficiency and is this characterized by low NPQ under drought? (2) Are these phenotypic
88 effects associated with transcriptomic changes? (3) Do these changes lead to modifications

89 in physiological processes with sedaxane applied as seed treatment? We integrated whole
90 plant physiological responses with changes in global gene expression in leaf tissues to obtain
91 more comprehensive understanding of the regulatory genetic mechanisms underlying the
92 physiological responses of SDHI treated plants under drought stress.

93 The focus of our investigation was the leaf as the main photosynthetic organ maximizing
94 carbon assimilation [15] and a major target for improving photosynthetic efficiency. However,
95 the root and pregerminated seed tissues were included in the gene co-expression and gene
96 network analysis to aid our understanding of the interactions regulating plant responses to
97 sedaxane under drought conditions because of translocation and systemic activity of
98 sedaxane into developing tissues following seed germination.

99

100

101 2. MATERIALS AND METHODS

102 2.1. Plant Growth Conditions and Experimental Design

103 Two experiments were carried out. Experiment 1 was used to measure sedaxane treated
104 plants for photosystem II efficiency and photosynthesis using detailed chlorophyll fluorescence
105 and gas exchange analysis. Experiment 2 was designed for transcriptomics analysis. Plant
106 tissues were collected for RNA isolation as soon as changes in PSII efficiency were confirmed
107 on indicator plants using portable fluorometer (Fluorpen FP100, Photon System Instruments,
108 Czech. Republic).

109 Winter wheat seed (cv. Gallant) were treated with Sedaxane at 10g a.i./100kg seed (Syngenta
110 Crop Protection UK, Cambridge) or left untreated. Untreated and treated seeds were initially
111 tested on potato dextrose agar medium (PDA) for any fungal or bacterial infection to ensure
112 that only healthy seeds were used in all experiments [16]. Plants were grown in a walk-in
113 growth chamber at the University of Nottingham with controlled temperature and light intensity
114 of 15°C and 300 $\mu\text{molm}^{-2}\text{s}^{-1}$, respectively. Photoperiod was maintained at 8 h light/16 h dark
115 throughout the course of the experiment. Seeds were pre - germinated on water moistened
116 filter paper for 2 d prior to planting into 9cm, 0.36L pots filled with either compost (John Innes
117 2, experiment 1) or γ -radiated loamy sand soil (experiment 2) prepared as described by
118 Sturrock et al. [17]. The amount of water in soil available to the plants at field capacity was
119 determined as described by Ajigboye et al. [11]. Water was initially supplied to 60% of
120 available water at full field capacity (AW_{FC}) and maintained at either 10% or 90% AW_{FC} .

121 Experiment 1 was designed as randomized block with two factors, fungicide treatment
122 (sedaxane treated or untreated) and soil moisture (90% or 10% available water at full field
123 capacity). There were seven replications of each treatment. Plants were divided into two
124 groups; "drought-stressed" and "non-stressed", each group with equal number of treated and
125 untreated seedlings. Water was withheld from the drought-stressed plants to attain 10%
126 available water at full field capacity (AW_{FC}) by 8 days after germination (DAG) while non-

127 stressed plants were supplied with sufficient water to attain 90% AW_{FC} at 3 DAG and
128 maintained at the same available water until the end of the experiment. Experiment 2 was
129 designed as randomized block with two treatments, sedaxane or untreated and consisted of
130 22 replicates, seven of which were considered as indicator plants while samples for RNA
131 isolation were collected from the remaining 15 replicates. All plants were maintained at 10%
132 AW_{FC} from 5 DAG.

133 **2.2. Experiment 1: Photosynthetic Efficiency and Growth Analysis**

134 The polyphasic rise in chlorophyll a fluorescence (OJIP) transient was measured using
135 portable fluorometer (Fluorpen FP100, Photon System Instruments, Czech Republic)
136 between 12-2pm daily from 9 to 11 DAG. Leaves were not dark adapted prior to obtaining
137 measurements. Therefore, we describe minimal and maximal fluorescence as F_o' and F_m' ,
138 respectively. OJIP transient was induced by strong light pulse of $3000 \mu\text{mol m}^{-2}\text{s}^{-1}$. Data
139 extracted along the recorded transient include fluorescence intensity at 50 μs , considered to
140 be minimal fluorescence F_o' , fluorescence intensity at J-step (2 ms), i-step (60 ms) and at
141 the peak of the transient P (= F_m'). F_v'/F_m' was computed as $[(F_m' - F_o')/F_m']$. Biophysical
142 parameters involving energy fluxes per reaction centers were automatically computed from
143 the transient curve using the JIP test as defined by Strasser et al [18]. Photosystem II
144 quantum yield was measured independently of the OJIP transient. Measuring light of 900
145 $\mu\text{mol m}^{-2}\text{s}^{-1}$, was applied to acquire minimal fluorescence F_o' followed by a saturating light
146 pulse of $3000 \mu\text{mol m}^{-2}\text{s}^{-1}$ to measure F_m' . QY is considered equivalent to $[F_v'/F_m']$ in light
147 adapted plants. All measurements were made on the youngest fully expanded leaf on each
148 plant.

149 At 12 DAG, light response of gas exchange and chlorophyll fluorescence were quantified
150 simultaneously using an infra-red gas analyzer, LI6400XT, equipped with leaf chamber
151 pulse-amplitude modulated fluorometer LI6400-40 (LI-COR, Lincoln, NE, USA). Leaves were
152 dark adapted in the growth chamber for 60 min prior to measurement by wrapping sections

153 of the leaf in low-weight silver aluminium foil. The dark-adapted leaves were placed in the
154 chamber, they were left for 5 min in the dark before F_0 was measured and then a saturating
155 pulse applied to measure F_m . At this point the actinic light was applied. In the light-adapted
156 state F_m' was measured by applying a saturating pulse of $7000 \mu\text{mol m}^{-2} \text{s}^{-1}$ (for 0.8 s). F_0'
157 was measured by switching off the actinic for 2 s after the saturating pulse and applying far-
158 red (FR) light. A series of illumination at PAR values was started at 0 and shifting to 2000,
159 waiting for 3 min at each light intensity before measurement. Fluorescence and gas
160 exchange parameters were calculated directly from the Licor software
161 (https://www.licor.com/env/products/photosynthesis/LI-6400XT/software_downloads.html).
162 Measurements were made under constant leaf temperature of 18°C , CO_2 concentration of
163 $400 \mu\text{l L}^{-1}$, relative humidity 50- 55%, gas flow rate $500 \mu\text{mol air s}^{-1}$ and photosynthetic photon
164 flux density (PPFD) of $1000 \mu\text{molm}^{-2}\text{s}^{-1}$.

165 Plant height was measured from the base of the plant to the tip of the longest leaf. Plants
166 were harvested 32 days after transplanting, fresh weights were measured before plants were
167 oven-dried at 80°C for 72 h to a constant weight. Dry weight was defined as dry weight/fresh
168 weight. Percentage water content was defined as (fresh weight – dry weight)/fresh weight.

169 **2.3. Experiment 2: Gene Expression Analysis**

170 **2.3.1. Sampling**

171 Chlorophyll (Chl) a fluorescence transient (OJIP) induced as described in experiment 1, was
172 measured daily on the fully expanded leaf on the main shoot of plants considered as indicator
173 plants from 5 DAG. OJIP was induced as described in experiment 1. As soon as significant
174 differences ($P < 0.05$) in PSII efficiency (F_v'/F_m') between treatments were detected in the
175 indicator plants at 9 DAG, leaf and root samples were collected individually from the remaining
176 15 replicates for RNA extraction.

177 **2.3.2. RNA Extraction**

178 Harvested tissues were immediately frozen in liquid nitrogen and stored at -80°C prior to
179 processing. Total RNA from leaf and roots of sampled plants as well as pre-germinated seeds
180 (2 d) was extracted from 100mg tissue. Frozen tissues were homogenized in TRIzol using a
181 FastPrep-24 (MP BIO) and lysing matrix D. Extracted RNA was then purified (RNeasy Mini
182 Kit, Qiagen). The extracted RNA was quantified with a NanoDrop ND-2000 UN-VIS
183 spectrophotometer (Thermo Scientific) and the integrity checked by fragment length on 2%
184 agarose gel electrophoresis.

185 **2.3.3. Microarray Experiments**

186 RNA from 3-5 individual plants was combined into one sample per treatment and replicate.
187 Eighteen arrays were used in total, representing two treatments, three tissue types and three
188 replicates. Hybridization of biotin-labelled RNA to Affymetrix Wheat GeneChip arrays and
189 array scanning were carried out at the University of Nottingham Affymetrix Microarray service
190 according to the manufacturer's instructions
191 (www.affymetrix.com/support/technical/manual/expression.manual.affx). Normalization and
192 analysis of differential expression was carried out using GeneSpring GX13 (Agilent
193 Technologies). Baseline preprocessing and normalization were carried out using the Robust
194 Multiarray Average summarization algorithm (RMA), as described by Irizarry et al. [19].
195 Tissues from the leaf root and pre-germinated seed were examined separately. A one-way
196 ANOVA with Benjamini Hochberg FDR multiple test correction was applied in order to select
197 genes that reveal significant changes ($P < 0.05$) in their expression. All treatments for the
198 tissues were compared with the control experiment of corresponding tissue. A cutoff value of
199 1.5-fold change was adopted to discriminate expression of genes that were differentially
200 expressed in response to sedaxane treatment.

201 **2.3.4. Gene Ontology Enrichment and Functional Pathway Analysis**

202 To categorize differentially expressed genes based on their biological functions, list of genes
203 identified by microarray analysis (≥ 1.5 -fold change) were submitted to MapMan for analysis

204 [20]. Transcripts were assigned into functional categories (or bins) of metabolism and cell
205 function. The Wilcoxon Rank Sum test corrected with Benjamini Hochberg FDR multiple test
206 was used to identify differentially regulated bins. Gene ontology enrichment of the gene lists
207 was carried out using the Parametric Analysis of Gene Set Enrichment (PAGE) in the
208 agriGO toolkit (<http://bioinfo.cau.edu.cn/agriGO/analysis.php>) [21]. Benjamini-Hochberg
209 multi-test adjustment method for the P-value was selected. P-value of 0.05 and false
210 discovery rate (FDR) <0.05 was used as a cutoff to select significantly enriched GO terms.

211 **2.3.5. Genome-scale gene network analysis**

212 A web-based Genome-scale gene network method was used. RMA normalized microarray
213 data were uploaded to the DeGNServer <http://plantgrn.noble.org/DeGNServer/Analysis.jsp>.
214 Networks with reduced edge densities were generated on the basis of co-expression (cut-off
215 >0.8) and Context Likelihood or Relatedness (CLR, at a cut-off of >3.6). The constructed
216 network and sub network were uploaded into Cytoscape [22] for visualization. The ranked
217 genes and common subgraphs of key differentially expressed genes were produced in both
218 the DEGNserver and Cytoscape. All the differential expressed genes of each set were
219 selected to build a sub-expression profile unit, and were implemented for correlation analysis
220 by value-based co-expression network method (gene association value). Considering the
221 computative speed and empirical accuracy comparison, z-scores value based co-expression
222 method and Spearman's rank correlation estimation method were applied in our analysis.

223 **2.3.6. qRT-PCR**

224 To validate the microarray experiment, RNA from microarray as well as from an independent
225 experiment was used for qRT-PCR. DNase treated RNA were from the microarray
226 experiment and from plants of a different seed lot grown under the same controlled
227 environmental conditions described earlier. qRT-PCR was performed for six genes from the
228 gene network analysis (Table S1). CFX96 (Bio-Rad, UK) was used for qPCR with iTaq™
229 Universal SYBR® Green one-step kit (Bio-Rad). Reactions consisted of 2 µL of 20 ng of total

230 RNA, 0.012 μ L of 300nM forward and reverse primers, 5 μ L of iTaq™ Universal SYBR®
231 Green reaction mix (2x), 0.125 μ L of iScript reverse transcriptase and 2.8 μ L of nuclease-
232 free water for a final reaction volume of 10 μ L. Reactions were under the following
233 conditions: 50°C for 10 min, 95°C for 1 min, then 40 cycles of 10 s at 95°C for denaturation
234 and 15 s at 60°C for annealing, extension and plate read. At the end of each reaction,
235 dissociation curve was performed from 65°C–95°C in 0.5°C increments for 0.05 s, which
236 confirmed a single peak for each set of primers. No-template controls were included for each
237 primer set per run to confirm the absence of contamination and primer dimer. No-template
238 control consistently recorded no signal or were significantly suppressed, with signals recorded
239 after 10 or more cycle threshold above the target signal. No-reverse transcription controls
240 were run for each RNA sample to confirm the absence of genomic DNA contamination. The
241 PCR reactions were performed in triplicates for each gene being validated. The
242 quantification cycle (Cq) for each type of PCR product were determined for all samples using
243 Bio-Rad CFX Manager 3.1 (Bio-Rad, UK). All Cq values were normalized to two reference
244 genes, Ubiquitin-conjugating enzyme and Cell division control protein, AAA-superfamily of
245 ATPases [23].

246 **2.4. Statistical analysis**

247 Analysis of variance (ANOVA) of chlorophyll fluorescence, and gas exchange parameters,
248 and biomass were performed with Genstat 16th Edition (VSN International). Treatments were
249 considered significantly different at Least Significant Difference (LSD) of 5% ($P \leq 0.05$).

250

251 3. RESULTS

252 3.1. Sedaxane Improves Wheat Photosynthetic Efficiency under Drought Stress

253 Conditions

254 We first used fast induction chlorophyll fluorescence (OJIP) transient to rapidly quantify
255 changes in chlorophyll fluorescence parameters measured on plants grown at 10% (drought-
256 stressed) and 90% (non-stressed) available water at field capacity (AW_{FC}). This technique
257 allowed us to monitor the efficiency of photosystem (PS) II of the youngest fully expanded leaf
258 of the primary plant tiller over a 3 d period. Across both treatments, there were no interactions
259 between sedaxane and water regime. The main effect of sedaxane treatment from 9 to 11
260 DAG on efficiency of PSII photochemistry (F_v/F_m'), quantum yield (QY) and dissipated energy
261 flux (Dlo/RC) are shown in Fig. 1. The efficiency of PSII photochemistry (F_v/F_m') increased
262 with sedaxane treatment from 9 DAG compared with the untreated control, with the highest
263 increase ($P < 0.05$) observed at 11 DAG (Fig. 1A). A similar trend was observed for QY (Fig.
264 1B). Dissipated energy flux (Dlo/RC) per PSII active reaction center was lower in plants grown
265 from sedaxane treated seeds from 9 DAG and remained lower (8% $P < 0.05$) than the untreated
266 plants 11 DAG (Fig. 1C). The above results showed that sedaxane had a significant impact
267 on PSII photochemistry. Therefore, we quantified the effect of sedaxane on the photosynthetic
268 performance of drought-stressed and non-stressed plants through simultaneous
269 measurement of leaf chlorophyll fluorescence (CF) and gas exchange parameters 12 DAG
270 under a range of incident light fluxes. Drought stress (10% AW_{FC}) at 12 DAG resulted in a
271 significant decrease in qP compared to non-stressed plants (90% AW_{FC}) at higher light
272 intensities above $750 \mu\text{mol m}^{-2}\text{s}^{-1}$ (Fig. 2). The rate of stomatal conductance under drought
273 stress declined by almost 17% ($P < 0.05$) at each light intensity compared to the non-stressed
274 control (Fig. S1A). A similar trend was observed for the rate of leaf transpiration although the
275 effect was significant ($P < 0.05$) under higher light intensities between 1200 to $2000 \mu\text{mol m}^{-2}$
276 s^{-1} (Fig. S1B). Sedaxane-treated plants under both water availability regimes had 8% lower
277 NPQ compared to untreated ($P < 0.05$) at high light intensities above $1000 \mu\text{mol m}^{-2} \text{s}^{-1}$ (Fig.

278 3A). Generally, under the range of incident light fluxes, the rate of photosynthesis was 10%
279 lower in drought-stressed plants than in non-stressed control. However, interactions between
280 fungicide and AW_{FC} treatment showed that photosynthesis was 8% higher in sedaxane-treated
281 plants grown under drought stress compared to untreated control ($P < 0.05$; Fig. 3B).

282 At 12 DAG no further interactions were detected between treatments and the main effects of
283 sedaxane or water availability on Φ_{PSII} , F_v/F_m and F_v'/F_m' were not significant at LSD of 5%
284 (data not shown).

285 Drought stress (10% AW_{FC}) 36 DAG significantly reduced ($P < 0.001$) tiller number by 78%
286 (Table 1). There were significant interactions between seed treatment and AW_{FC} for plant
287 height, total percentage water content and dry weight. Under drought stress, sedaxane
288 increased plant height by 7% ($P = 0.044$), reduced percentage water content ($P = 0.027$) and
289 increased dry weight by 37%, ($P = 0.027$) compared to untreated control.

290 **3.2. Microarray Analysis of Sedaxane-Responsive Genes**

291 We showed that photosynthetic efficiency, photosynthesis and biomass increased in wheat
292 plants from sedaxane treated seeds under drought conditions. To further understand the
293 molecular basis of the observed physiological effects, we performed microarray analysis
294 (Wheat GeneChips; Affymetrix) to determine gene expression. Genes were considered
295 differentially regulated if their expression was significantly different from the untreated control
296 ($P < 0.05$). A total number of 4369 differentially regulated genes (adjusted P value of < 0.05)
297 were identified and we used a minimum cut-off of 1.5-fold change to identify genes that were
298 robustly regulated by sedaxane (Table S2). The number of genes differentially regulated in
299 response to sedaxane was 2200 in leaves (898 up-regulated and 1302 down-regulated), 514
300 in roots (237 up-regulated and 271 down-regulated) and 2066 in pre-germinated seeds (615
301 up-regulated and 1452 down-regulated). Comparison of the microarray data from all of the
302 three tissues did not show any up-or down-regulated (Fig. 4), however less than 3% of the
303 differentially expressed genes overlapped between any two tissues. Thus, most of the

304 regulated genes were tissue specific, indicating that pre-germinated seeds, leaves or root
305 tissues respond to sedaxane by activating distinct sets of genes.

306 **3.3. Functional Classification of Sedaxane Responsive Genes with Altered** 307 **Expression**

308 MAPMAN software [20] was used to gain insight into the biological processes affected by
309 sedaxane in each of the three tissues considered (Table 2 & 3; $P < 0.05$, Wilcoxon rank sum
310 test in the MapMan tool). In the overview of cell function, analysis of differential gene
311 expression in pregerminated seeds revealed a down-regulation of genes assigned to the
312 categories DNA synthesis/chromatin structure encoding core histone H2A/H2B/H3/H4 domain
313 containing protein and biotic stress generally encoding genes associated with disease
314 resistance proteins, HEVEIN FAMILY PROTEIN, PATHOGENESIS-RELATED (PR)
315 PROTEINS although majority of genes in the seeds were unassigned (Tables 2 & Table S3A).
316 In roots, genes involved in biotic stress such as those encoding the PATHOGENESIS-
317 RELATED PROTEINS and DEFENSIN-LIKE PROTEINS were down regulated. (Tables 2 &
318 Table S3B). In the leaf, an overview of the transcriptional responses affecting genes coupled
319 to cell function showed that genes connected to protein synthesis were up-regulated (Table 2
320 & Table S3C). These up-regulated genes encode the various sub units (30S, 40S, 50S and
321 60S) of ribosomal protein from the chloroplasts. In contrast, genes involved in hormone
322 metabolism, signaling and biotic stress were generally down regulated (Table 2 & Table S3C).
323 For example, in pathways involved in hormone metabolism, genes encoding jasmonate
324 biosynthetic precursors, ethylene, auxin and abscisic acids were down-regulated. Similarly,
325 most of the genes involved in signaling were down-regulated, including genes associated with
326 CALCIUM SIGNALING, MITOGEN-ACTIVATED PROTEIN KINASES, LEUCINE RICH
327 REPEAT PROTEIN KINASES FAMILY PROTEIN, although two genes associated with light
328 signaling, encoding the EARLY LIGHT INDUCIBLE PROTEIN HV58, known to function
329 against chlorophyll induced oxidative damage [24] were activated. In the stress category,

330 genes encoding defense related proteins and PR-proteins were generally down regulated
331 except a dirigent-like protein which was upregulated (Table S3C).

332 In the overview of metabolism, enriched functional categories were detected in the leaf
333 tissue only (Table 3). It is likely that several important transcripts which can exert significant
334 changes in downstream gene expression to lead to a substantial biological effect were
335 eliminated [25] in pregerminated seeds and roots due to our stringent criteria (fold change
336 ≥ 1.5). A closer look at the categories showed that genes involved in cell wall modification
337 and tetrapyrrole synthesis categories were up-regulated (Table 3; Table S4). Upregulated
338 genes related to cell wall modifications include the cell wall loosening EXPANSINS and cell
339 wall-strengthening enzymes, XYLOGLUCAN ENDOTRANSGLYCOSYLASES (XTHs, Table
340 S4). The set of genes involved in tetrapyrrole synthesis include those encoding chlorophyll
341 precursors corresponding with the various steps in chlorophyll biosynthesis including
342 DELTA-AMINOLEVULINIC ACID DEHYDRATASE, UROPORPHYRINOGEN
343 DECARBOXYLASE, PROTOPORPHYRINOGEN IX OXIDASE, MG-PROTOPORPHYRIN IX
344 and PROTOCHLOROPHYLLIDE REDUCTASE (Table S4).

345 We also explored changes in the abundance of transcripts from genes that mediate known
346 biological processes and molecular function in the tissues using the Parametric Analysis of
347 Gene Enrichment Analysis (PAGE) tool of agriGO [21]. Results showing the most enriched
348 GO terms from these analyses are shown in Table 4 and 5. In pregerminated seeds, GO
349 analysis identified molecular functions that were significantly enriched in up-regulated genes
350 with the terms glutathione transferase activity and cofactor binding while down-regulated
351 genes were enriched in DNA binding (Table 4). For biological processes, the most significantly
352 enriched biological process was glutathione metabolic processes and nucleosome assembly
353 for up-regulated and down regulated genes respectively (Table 4). There were no significantly
354 enriched GO terms in the root. In the leaf, molecular functions with highly enriched GO terms
355 for up-regulated genes were ribosomal RNA binding, GTP binding, structural constituent of
356 ribosome and transferase activity while down-regulated genes enriched GO terms were

357 related to protein serine/threonine kinase activity and co-enzyme binding (Table 5). Enriched
358 GO terms involved in biological processes for up-regulated genes were translation, ribosome
359 biogenesis and chlorophyll metabolic process and significantly enriched categories for down-
360 regulated genes were jasmonic acid biosynthetic process, defense response and response to
361 other organisms (Table 5).

362 **3.4. Co-expression and Gene Regulatory Network Analysis**

363 We analyzed co-expressed genes to identify the functional associations between sedaxane
364 responsive genes that are part of the same biological process and may be under similar
365 transcriptional control in all three different tissues. To identify genes associated with stress,
366 we submitted the top 10 up/down-regulated genes as seed genes to exact sub-networks, the
367 sub-networks were visualized with the DEGNServer and Cytoscape. The centrality to co-
368 expression networks of hubs tend to be associated with essential roles in biological processes
369 [26],[27]. Forty genes with the highest stress centrality followed by degree centrality (Fig. 5
370 and Table S5) were annotated using the PLEXdb annotation portal [28] and HarvEST (version
371 1.59). About 75% of the top genes were upregulated in the leaf, while only about 50% and
372 35% were upregulated in the root and pregerminated seeds respectively (Table S5). Among
373 differentially induced genes associated with drought tolerance in the leaf and roots but down
374 regulated in the pre-germinated seeds, were AQUAPORIN, CHOLINE DEHYDROGENASE,
375 HESSIAN FLY RESPONSE GENE 1 PROTEIN, DIRIGENT LIKE PROTEIN (DIR), ZINC
376 FINGER PROTEIN, 2-OXOGLUTARATE DEPENDENT OXYGENASE and DEHYDRIN. An
377 exception to the group is the TYPE 1 NON SPECIFIC LIPID TRANSFER PROTEIN (nsLTPs),
378 XYLOGLUCAN ENDOTRANSGLYCOSYLASES (XTHs) and WAX2 protein which were
379 upregulated only in the leaf tissues. The GLYCINE-RICH PROTEIN (GRPs), MALTO-
380 OLIGOSYLTREHALOSE TREHALOHYDROLASE, TRANSCRIPTIONAL REGULATOR
381 LYSR, FRUCTAN EXOHYDROLASE and CYSTEINE SYNTHASE were among the down
382 regulated genes in the leaf.

383 Six of the top genes with high stress and degree centrality (HFR1 and DIR, nsLTPs GRP –
384 like, XTHs and an unknown gene *TaAffx.30098.1.S1_at*) were selected for qRT-PCR analysis
385 in the leaf tissue (Table S4 and Table S5). Excess RNA produced during microarray target
386 preparation and from an independent experiment was used separately to provide template for
387 qRT-PCR. The expression ratios produced by qRT-PCR and the microarray experiments were
388 similar (Fig. 6), and except for the gene encoding GRPs, all the genes were confirmed as
389 preferentially upregulated in leaf by both the microarray and qRT-PCR.

390

391 **4 DISCUSSION**

392 Sedaxane applied as seed treatment induced significant increase in the efficiency of
393 excitation energy capture by open PSII reaction centers (F_v'/F_m') in drought stressed plants.
394 This is in agreement with previous studies showing similar effect exerted by another SDHI,
395 isopyrazam, shown to enhance the photosynthetic efficiency of disease-free wheat plants
396 under drought conditions [11]. Changes in F_v'/F_m' and Df_o/RC were used in this study as
397 early indicators of modifications in PSII operating efficiencies attributed to thermal dissipation
398 of excessive excitation energy in the light harvesting complexes of PSII, estimated as non-
399 photochemical quenching or NPQ [29]. Under stress conditions, NPQ acts as a
400 photoprotective mechanism by which PSII activity is down-regulated to prevent damage to
401 PSII reaction centers. Consequently, decrease in NPQ accompanied with an increased rate
402 of leaf photosynthesis in sedaxane treated plants under drought conditions suggests that
403 sedaxane treatment led to preferential allocation of excitation energy into photochemical
404 processes [30].

405 Sedaxane inhibits the succinate dehydrogenase (SDH) complex II in the fungal mitochondria
406 and there is a possibility that similar effect may be exerted on the plant mitochondrial
407 complex II although this hypothesis was not tested in the present study. Inhibition of SDH by
408 partial reduction of SDH subunits has been reported previously to improve leaf
409 photosynthesis and biomass by increasing stomatal conductance in tomato and *Arabidopsis*
410 [31],[32]. Acevedo et al [33] recently reported that an SDH flavoprotein subunit (*SDH1-like*)
411 transcript was upregulated in *Ilex paraguariensis* plants exposed to drought. This authors
412 showed that increase in *SDH1-like* transcripts correlated with elevated ABA concentration.
413 ABA accumulates in the guard cells of drought stressed plants to induce stomatal closure
414 and conserve water. In the present study, genes encoding ABA were downregulated in
415 sedaxane treated plants under drought. In addition, we detected interactions between
416 sedaxane and AW_{FC} on stomatal conductance which were significant at 10% LSD (results
417 not shown), suggesting that, treatment with sedaxane may have contributed to the

418 maintenance of stomata function under drought consistent with our observations of improved
419 photosynthesis, increased biomass and reduced water content of sedaxane-treated wheat
420 seedlings.

421 **Transcriptome Response to Sedaxane in Plant Tissues**

422 In total, 4369 genes, around 7% of the genes present on the chip were found to be differentially
423 expressed ($P < 0.05$) in response to sedaxane seed treatment in all three tissues considered
424 under drought conditions. About 50 % (≥ 1.5 -fold change) of the differentially expressed genes
425 (DEGs) were found in leaves and pregerminated seeds, while only 12% were found in the
426 roots. When comparing DEGs in the three tissues collectively, no common DEGs were
427 identified. However, about 3% DEGs overlapped in the leaf and pregerminated seed, and less
428 than 1% in the leaf and root or the pregerminated seed and root tissues. Hence, distinct sets
429 of genes were generally activated in individual tissues of drought stressed wheat seedlings in
430 response to sedaxane. Our work thus offers the first comprehensive picture of transcriptional
431 changes triggered by an SDHI, sedaxane, in distinct tissues of drought-stressed wheat plants
432 associated with increased PSII efficiency and photosynthesis.

433 **4.2. Cellular and Metabolic Responses to Sedaxane**

434 **4.2.1 Pregerminated seeds and Roots**

435 No drought stress was introduced to the pregerminated seeds in this study; therefore, we
436 consider gene differential expression in this tissue a direct effect of sedaxane seed treatment
437 under non-stress conditions. Upregulated genes in response to sedaxane were significantly
438 enriched in glutathione-s-transferase (GST) activity. GSTs are important proteins involved in
439 efficient scavenging of plant toxins such as ROS, which accumulate as a consequence of
440 increased oxidative stress [34] and thus maintain redox homeostasis in plant tissues [35].
441 Our results showed that the transcripts of these ROS scavenging proteins, GSTs
442 accumulated during germination, to suggest a close association between sedaxane seed
443 treatment protection of the plant (leaf) from oxidative stress under drought conditions.

444 Pathway analysis of all differentially expressed genes in the root showed that biotic stress
445 was the only enriched pathway (Table 2). These genes encode pathogenesis-related
446 proteins and defensin-like proteins, generally upregulated in response to pathogen attack
447 which ultimately impede further pathogen invasion and enhance the capacity of the host to
448 limit subsequent pathogen infection [36],[37]. Interestingly, many pathogenesis-related
449 genes are also induced upon exposure of a plant to abiotic stress ensuring disease
450 resistance [38]. In our study, all the genes in this category were downregulated suggesting
451 treated roots were not exhibiting biotic stress related responses under drought possibly due
452 to the protective properties of sedaxane.

453 **4.2.2 Leaves**

454 4.2.2.1 Jasmonate Biosynthesis and Signaling

455 Early plant responses to drought involve the adjustment of the levels of endogenous hormones
456 to activate physiological pathways for adaptation, thereby modulating the expression of genes
457 involved in processes relating to PSII, photosynthesis, cell modification, growth and
458 development under abiotic stress conditions [39]-[41]. Hormone metabolism was one of the
459 enriched pathways involved in key cellular functions in our study in particular genes involved
460 in the jasmonate synthesis. This is substantiated by GO analysis showing enrichment for
461 genes involved in jasmonic acid biosynthetic and metabolic processes (Table 5). JAs have
462 been shown to play critical role in the early priming (preconditioning stage) to moderate
463 drought in *Arabidopsis* (*Arabidopsis thaliana*), stimulating preparatory response for drought
464 acclimation (for example stomatal closure and cell wall modification) [42]. Our datasets show
465 that genes encoding the various derivatives of jasmonates among which are jasmonic acid
466 and genes encoding enzymes involved in the biosynthetic pathway including allene oxide
467 synthase, allene oxide cyclase; lipoxygenase and 12-oxophytodienoic reductase were
468 downregulated. Under drought stress conditions in sedaxane treated plants, the JA-signaling
469 genes involved in calcium signaling and mitogen-activated protein kinases were also
470 downregulated. Calcium ion influx (Ca^{2+}) and mitogen-activated protein kinases are key

471 components of JA signal transduction, accumulating in response to abiotic and biotic stress
472 [43],[44]. Treatment with JA has been shown to induce cytosolic free-Ca²⁺ concentration
473 ([Ca²⁺] cyt) in *Arabidopsis thaliana* leaves [45]. However, high concentrations of JA inhibit cell
474 expansion and cell wall modification and reduce plant growth [46],[47]. Thus downregulation
475 of JA biosynthesis and signaling under drought stress in sedaxane treated plants is likely to
476 act to establish new homeostasis through altered signaling and redirection of metabolism from
477 defense/stress responses towards modification of plant growth and development.

478 4.2.2.2 Cell Wall Modifications

479 Physical properties of the cell wall play a crucial role in the response of plants to drought [48].
480 Expansins mediate cell wall -loosening factors that directly induce turgor-driven cell wall
481 extension [49]. Secondary wall-loosening enzymes such as xyloglucan
482 endoglycosylase/hydrolases (XTHs) modify the structures of the cell wall, aiding cell wall
483 loosening [50],[51]. Our microarray and qRT-PCR analyses showed upregulation of genes
484 encoding cell-wall-loosening expansins and XTHs thus indicating that sedaxane is likely to
485 confer adaptive responses to drought stress facilitating cellular expansion and modification of
486 shoot growth and development. Upregulation of expansins genes have been implicated in
487 increased drought tolerance in plants [42],[52].

488 4.2.2.3 Tetrapyrrole biosynthesis

489 The tetrapyrrole biosynthetic pathway is responsible for the synthesis of different types of
490 porphyrins in higher plants including chlorophyll and heme essential for several primary
491 metabolic processes [53]. The major site of tetrapyrrole biosynthesis in plants occurs in
492 plastids except the last steps of heme biosynthesis, which are possibly localized in both
493 mitochondria and plastids [53]. In this study, expression of genes encoding various
494 intermediates of the tetrapyrrole biosynthesis pathway was strongly upregulated in sedaxane
495 treated plants suggesting that these plants were able to maintain a flux through the tetrapyrrole
496 pathway under drought conditions. High level of tetrapyrrole intermediates has been

497 previously associated with improved drought tolerance in transgenic rice
498 expressing *Myxococcus xanthus* protoporphyrinogen oxidase [54],[55]. Insertion of Mg²⁺ into
499 Protoporphyrin- IX by the enzyme Mg-chelatase was shown to favor the chlorophyll branch of
500 the pathway [56]. In our data, genes encoding enzymes Magnesium-chelatase subunit and
501 Mg-protoporphyrin IX, precursors for chlorophyll biosynthesis were upregulated. In plants, the
502 protochlorophyllide reductase oxidoreductase (POR) step in tetrapyrrole pathway is strictly
503 light-dependent, as it requires protochlorophyllide to be activated by light [57],[58]. In
504 illuminated plants, protons are translocated from the stroma into the intra thylakoid lumen [59].
505 This movement is coupled with the release of Mg²⁺, into the stroma. These ion fluxes are
506 known to contribute to an increase of the pH of the stroma from 7 to 8, an optimum pH of most
507 enzymes involved in the Benson- Calvin cycle [60],[61], including rubisco, fructose-1,6-
508 bisphosphatase, sedoheptulose-1,7-bisphosphatase, and phosphoribulokinase. Hence, the
509 light-mediated increase of Mg²⁺ and H⁺ enhances the activity of key enzymes of the Calvin-
510 Benson cycle. This coupled with the observed increased rate of photosynthesis would indicate
511 a maintained balance between PSII activity and the Calvin cycle, thus protecting the PSII from
512 photo damage.

513 Based on our results, the tetrapyrrole biosynthetic pathway is likely to be the target of
514 sedaxane in wheat metabolism, driven by the production of glutamate in the mitochondria.
515 Glutamate, the precursor for the synthesis of tetrapyrroles in plants is formed from 2-
516 oxoglutarate and glutamine. 2-Oxoglutarate mainly produced in the mitochondria and
517 transported to the chloroplast is an obligatory substrate for 2-oxoglutarate-dependent
518 dioxygenases [62] and a key metabolite required for ammonia assimilation [63]. In this study,
519 one of the upregulated top genes encode 2-oxoglutarate- dependent oxygenase. In addition,
520 the tetrapyrrole intermediate Mg-protoporphyrin IX has been postulated to act as a signal
521 molecule in signaling pathways between the chloroplast, nucleus and the mitochondria, and
522 the accumulation of this metabolite is required to regulate the expression of genes encoding
523 proteins associated with photosynthesis [64],[65].

524 4.3. Central Players in the Sedaxane Regulated Network

525 We aimed to identify a hub subnetwork to provide more insight on the physiological impact of
526 sedaxane under drought conditions and ultimately to identify transcription factors that can
527 potentially be used as candidate genes to improve photosynthetic performance of wheat. We
528 used datasets from the leaves, roots and pregerminated seeds to identify 40 genes using
529 inferred network stress and degree centralities, computed for each of the coexpressed
530 regulatory genes in the network.

531 Our data suggest that dirigent proteins play a central role in protecting wheat plants against
532 the effects of severe drought through their impact on mechanical strength and flexibility of cell
533 wall. DIR-like family proteins have been implicated in cell wall lignin biosynthesis, which are
534 structural cell wall components of vascular tissues [66]. The hub with the highest stress
535 centrality in our network encoded the Hessian fly responsive protein 1 (HFR1), highly
536 upregulated in the leaf and root, also considered a dirigent-like protein involved in modulating
537 plant response to biotic stress [67] and previously implicated in cell wall strengthening via
538 deposition of phenolics [68] and secretion of protective surface waxes [69].

539 Increased dry weight has been associated with accumulation of cell wall expansin [47]. One
540 of the top ranked genes in the hub of the network encoded xyloglucan endotransglycosylase
541 (XTH), involved in strengthening and cell wall plasticity leading to water uptake in leaves under
542 drought conditions [51],[70]. The enrichment of pathways involved in cell wall modification,
543 and upregulation of genes encoding XTHs and expansins in the leaf is an indication that, the
544 selective loosening and strengthening of the cell wall in growing plant tissue under drought
545 conditions is likely to stimulate water uptake to increase growth and development in the plant
546 [71] which is consistent with increased dry weight in sedaxane treated plants under drought
547 stress. A proline-rich protein precursor was also upregulated. Recent discoveries point out
548 that proline is a key determinant of many cell wall proteins that plays important roles in plant
549 growth and development. Interestingly, a gene encoding aquaporin, involved in regulating

550 water movement across cell membranes [72] was also upregulated in both leaf and root
551 tissues. This suggests that water movement and use under drought conditions was enhanced
552 with sedaxane treatment consistent with the physiological phenotype of increased
553 photosynthesis and growth as well as reduction in NPQ of fungicide treated plants.

554 A gene hub encoding the calmodulin binding protein (CaM) was upregulated in both the leaf
555 and pregerminated seeds. CaM is small Ca^{2+} - sensing protein that acts as signal transducer
556 in a wide array of physiological processes including drought stress in plants [73],[74]. Using
557 knockout mutants of the CaM transcription factors (CAMTAs), Pandey et al [75] showed that
558 CaM was positively involved in drought stress tolerance in Arabidopsis. A new family of CaM-
559 binding proteins, the type 1 non-specific lipid transfer proteins (nsLTPs) was identified in
560 Arabidopsis [76]. In this study, we identified three hub genes encoding the nsLTPs, all
561 upregulated in the leaf tissue. nsLTPs also act as wax transporters, able to transfer lipids and
562 fatty acids across different membranes and are induced under drought stress [77]. nsLTPs
563 have been shown to be involved in epicuticular wax or cuticle biosynthesis [78]. Kottapalli et
564 al. [79] showed that epicuticular wax content increased in drought tolerant genotype of peanut
565 (*Arachis hypogaea*). Loss of epicuticular wax has been associated with increased water loss
566 in plants. In our study, one of the identified hub gene, the wax biosynthesis annotated as
567 Ecriferum 1 (CER1) and WAX2-like protein (WAX2) was also upregulated.

568 Another interesting gene in the network which plays a regulatory role in signaling and abiotic
569 stress tolerance is a transcriptional factor for glycine rich proteins (GRPs) [80]. The expression
570 of GRP genes is modulated by plant hormones, which in turn regulate plant growth,
571 development and stress responses [81]-[83]. In our study, GRP hub of genes was
572 downregulated whereas GRPs have been shown to accumulate under drought [84].

573 **4.4. CONCLUSION**

574 This study showed that the SDHI sedaxane, applied as seed treatment, improved PSII
575 efficiency, photosynthesis and biomass production of wheat under drought. These effects

576 were accompanied by low NPQ, as a result of a homeostasis between PSII activity and the
577 Calvin cycle.

578 Transcriptomic analysis suggests that sedaxane enhances wheat seedling
579 tolerance/resistance to drought stress by altering the expression of key genes/transcriptional
580 factors from seed germination. We propose a schematic of the effects of sedaxane on plant
581 physiology (Fig. 7) associated with differential patterns of nsLTPs, XTHs, CaM, HFR1, Zinc
582 finger protein 1 known to regulate the expression of drought tolerance/resistance traits in
583 crops. Initial responses were first observed in pregerminated seeds, where ROS scavenging
584 genes were upregulated involved in the reduction of oxidative stress. In the root, defense-
585 related genes were downregulated most likely to allow metabolites to be redirected towards
586 adaptive development. The most differentially expressed genes were observed in leaves
587 characterized by downregulation of jasmonate biosynthesis and signaling and increased
588 chlorophyll biosynthesis allowing for the remobilization of assimilates from stress-related
589 responses towards modified growth and development.

590 **ACKNOWLEDGEMENTS**

591 This research was funded by Syngenta grant RK3537. We thank Dr Guillermina Mendiando
592 for assistance with qRT-PCR.

593 **Competing interests**

594 The authors declare that they have no competing interests.

595

596

597

598 **LITERATURE CITED**

- 599 [1] J.S. Boyer, Productivity and Environment, *Science* 218 (1982) 443–448. B
- 600 [2] N.R. Baker, Chlorophyll Fluorescence: A Probe of Photosynthesis In Vivo, *Annu.*
601 *Rev. Plant Biol.* 59 (2008) 89–113.
- 602 [3] N.R. Baker, E. Rosenqvist, Applications of chlorophyll fluorescence can improve crop
603 production strategies: an examination of future possibilities, *J. Exp. Bot.* 55 (2004)
604 1607–1621. doi:10.1093/jxb/erh196.
- 605 [4] A.R. Reddy, K.V. Chaitanya, M. Vivekanandan, Drought-induced responses of
606 photosynthesis and antioxidant metabolism in higher plants, *J. Plant Physiol.* 161
607 (2004) 1189–1202. doi:10.1016/j.jplph.2004.01.013.
- 608 [5] M. Ashraf, P.J.C. Harris, Photosynthesis under stressful environments: An overview,
609 *Photosynthetica* 51 (2013) 163–190.
- 610 [6] A.V. Ruban, M.P. Johnson, C.D.P. Duffy, The photoprotective molecular switch in the
611 photosystem II antenna, *Biochim. Biophys. Acta - Bioenerg.* 1817 (2012) 167–181.
612 doi:10.1016/j.bbabi.2011.04.007.
- 613 [7] E.H. Murchie, K.K. Niyogi, Manipulation of photoprotection to improve plant
614 photosynthesis, *Plant Physiol.* 155 (2011) 86–92. doi:10.1104/pp.110.168831.
- 615 [8] B. Demmig-Adams, W.W. Adams, U. Heber, S. Neimanis, K. Winter, A. Krüger, F.C.
616 Czygan, W. Bilger, O. Björkman, Inhibition of zeaxanthin formation and of rapid
617 changes in radiationless energy dissipation by dithiothreitol in spinach leaves and
618 chloroplasts, *Plant Physiol.* 92 (1990) 293–301. doi:10.1104/pp.92.2.293.
- 619 [9] S. Hubbart, O.O. Ajigboye, P. Horton, E.H. Murchie, The photoprotective protein
620 PsbS exerts control over CO₂ assimilation rate in fluctuating light in rice, *Plant J.* 71
621 (2012) 402–412. doi:10.1111/j.1365-3113.2012.04995.x.
- 622 [10] Y. Fracheboud, J. Leipner, Practical applications of chlorophyll fluorescence in plant
623 biology, in: J.R. DeEll, P.M.A. Toivonen (Eds.), Springer US, Boston, MA, 2003: pp.
624 125–150. doi:10.1007/978-1-4615-0415-3_4.

- 625 [11] O.O. Ajigboye, E. Murchie, R. V. Ray, Foliar application of isopyrazam and
626 epoxiconazole improves photosystem II efficiency, biomass and yield in winter wheat,
627 Pestic. Biochem. Physiol. 114 (2014) 52–60.
- 628 [12] C.A. Berdugo, U. Steiner, H.-W. Dehne, E.-C. Oerke Effect of bixafen on senescence
629 and yield formation of wheat, Pestic. Biochem. Physiol. 104 (2012) 171–177.
- 630 [13] H.F. Avenot, T.J. Michailides, Progress in understanding molecular mechanisms and
631 evolution of resistance to succinate dehydrogenase inhibiting (SDHI) fungicides in
632 phytopathogenic fungi, Crop Prot. 29 (2010) 643–651.
633 doi:10.1016/j.cropro.2010.02.019.
- 634 [14] R. Zeun, G. Scalliet, M. Oostendorp, Biological activity of sedaxane – a novel broad-
635 spectrum fungicide for seed treatment, Pest Manag. Sci. 69 (2013) 527–534.
636 doi:10.1002/ps.3405.
- 637 [15] X.G. Zhu, S.P. Long, D.R. Ort, Improving photosynthetic efficiency for greater yield.
638 In S. Merchant, W.R. Briggs, and D. Ort, (eds), Annu. Rev. Plant Biol. 61 (2010) 235–
639 261.
- 640 [16] R. Ren, X. Yang, R. V. Ray, Comparative aggressiveness of *Microdochium nivale*
641 and *M. Majus* and evaluation of screening methods for *Fusarium* seedling blight
642 resistance in wheat cultivars, Eur. J. Plant Pathol. 141 (2014) 281–294.
- 643 [17] C.J. Sturrock, J. Woodhall, M. Brown, C. Walker, S.J. Mooney, R. V Ray, Effects of
644 damping-off caused by *Rhizoctonia solani* anastomosis group 2-1 on roots of wheat
645 and oil seed rape quantified using X-ray Computed Tomography and real-time PCR,
646 Front. Plant Sci. 6 (2015). doi:10.3389/fpls.2015.00461.
- 647 [18] R. Strasser, a Srivastava, M. Tsimilli-Michael, The fluorescence transient as a tool to
648 characterize and screen photosynthetic samples, Probing Photosynthesis:
649 Mechanism, Regulation & Adaptation (2000) 445–483.
- 650 [19] R.A. Irizarry, Exploration, normalization, and summaries of high density
651 oligonucleotide array probe level data, Biostatistics 4 (2003) 249–264.

- 652 [20] O. Thimm, O. Blasing, Y. Gibon, A. Nagel, S. Meyer, P. Kruger, J. Selbig, L.A. Muller,
653 S.Y. Rhee, M. Stitt, MAPMAN: a user-driven tool to display genomics data sets onto
654 diagrams of metabolic pathways and other biological processes, *Plant J.* 37 (2004)
655 914–939.
- 656 [21] Z. Du, X. Zhou, Y. Ling, Z. Zhang, Z. Su, AgriGO: a GO analysis toolkit for the
657 agricultural community, *Nucleic Acids Res.* 38 (2010) 64–70.
- 658 [22] M.E. Smoot, K. Ono, J. Ruscheinski, P.L. Wang, T. Ideker, Cytoscape 2.8: new
659 features for data integration and network visualization, *Bioinformatics* 27 (2011) 431–
660 432
- 661 [23] A.R. Paolacci, O.A. Tanzarella, E. Porceddu, M. Ciaffi, Identification and validation of
662 reference genes for quantitative RT-PCR normalization in wheat, *BMC Mol. Biol.* 10
663 (2009) 1–27. doi:10.1186/1471-2199-10-11.
- 664 [24] C. Hutin, L. Nussaume, N. Moise, I. Moya, K. Kloppstech, M. Havaux, Early light-
665 induced proteins protect Arabidopsis from photooxidative stress, *Proc. Natl. Acad.*
666 *Sci. U. S. A.* 100 (2003) 4921–6. doi:10.1073/pnas.0736939100.
- 667 [25] W.J. Chen, T. Zhu, Networks of transcription factors with roles in environmental
668 stress response, *Trends Plant Sci.* 9 (2004) 591–6.
669 doi:10.1016/j.tplants.2004.10.007.
- 670 [26] H. Jeong, S.P. Mason, A.-L. Barabasi, Z.N. Oltvai, Lethality and centrality in protein
671 networks, *Nature.* 411 (2001) 41–42.
- 672 [27] M.R.J. Carlson, B. Zhang, Z. Fang, P.S. Mischel, S. Horvath, S.F. Nelson, Gene
673 connectivity, function, and sequence conservation: predictions from modular yeast
674 co-expression networks, *BMC Genomics.* 7 (2006) 40. doi:10.1186/1471-2164-7-40.
- 675 [28] S. Dash, J. Van Hemert, L. Hong, R.P. Wise, J.A. Dickerson, PLEXdb: gene
676 expression resources for plants and plant pathogens, *Nucleic Acids Res.* 40 (2012)
677 D1194-201. doi:10.1093/nar/gkr938.

- 678 [29] N.R. Baker, A possible role for photosystem II in environmental perturbations of
679 photosynthesis, *Physiol. Plant.* 81 (1991) 563–570. doi:10.1111/j.1399-
680 3054.1991.tb05101.x.
- 681 [30] M. Brestic, G. Cornic, M.J. Freyer, N.R. Baker, Does photorespiration protect the
682 photosynthetic apparatus in french bean leaves from photoinhibition during drought
683 stress? *Planta* 196 (1995) 450–457. doi:10.1007/BF00203643.
- 684 [31] W.L. Araujo, A. Nunes-Nesi, S. Osorio, B. Usadel, D. Fuentes, R. Nagy, I. Balbo, M.
685 Lehmann, C. Studart-Witkowski, T. Tohge, E. Martinoia, X. Jordana, F. M. DaMatta,
686 A.R. Fernie, Antisense inhibition of the iron-sulphur subunit of succinate
687 dehydrogenase enhances photosynthesis and growth in tomato via an organic acid-
688 mediated effect on stomatal aperture, *Plant Cell* 23 (2011) 600-627.
- 689 [32] D. Fuentes, M. Meneses, A. Nunes-Nesi, W.L. Araujo, R. Tapia, I. Gómez, L.
690 Holuigue, R.A. Gutiérrez, A.R. Fernie, X. Jordana A deficiency in the flavoprotein of
691 Arabidopsis mitochondrial complex II results in elevated photosynthesis and better
692 growth in nitrogen-limiting conditions, *Plant Physiol.* 157 (2011) 1114-1127.
- 693 [33] R.M. Acevedo , S.J. Maiale , S.C. Pessino , R. Bottini , O.A. Ruiz , P.A. Sansberro,
694 A succinate dehydrogenase flavoprotein subunit-like transcript is upregulated in *Ilex*
695 *paraguariensis* leaves in response to water deficit and abscisic acid, *Biochemistry* 65
696 (2013) 48-54.
- 697 [34] K.A. Marrs, the functions and regulation of glutathione s-transferases in plants, *Annu.*
698 *Rev. Plant Phys.* 47 (1996) 127–158.
- 699 [35] C.H. Foyer, G. Noctor, Redox homeostasis and antioxidant signaling: a metabolic
700 interface between stress perception and physiological responses, *Plant Cell* 17
701 (2005) 1866–1875
- 702 [36] R.N. Goodman, A.J. Novacky, The hypersensitive reaction in plants to pathogens. A
703 resistance phenomenon, American Phytopathological Society Press St. Paul, MN
704 (1994).

- 705 [37] L.C. Van Loon, Induced resistance in plants and the role of pathogenesis-related
706 proteins. *Eur. J. Plant Pathol.* 103 (1997) 753–765
- 707 [38] P.J. Seo, M.J. Kim, J.-Y. Park, S.-Y. Kim, J. Jeon, Y.-H. Lee, J. Kim, C.-M. Park,
708 Cold activation of a plasma membrane-tethered NAC transcription factor induces a
709 pathogen resistance response in *Arabidopsis*, *Plant J.* 61 (2010) 661–671.
- 710 [39] A.G. Dobrikova, R.S. Vladkova, G.D. Rashkov, S.J. Todinova, S.B. Krumova, E.L.
711 Apostolova, Effects of exogenous 24-epibrassinolide on the photosynthetic
712 membranes under non-stress conditions., *Plant Physiol. Biochem.* 80 (2014) 75–82.
713 doi:10.1016/j.plaphy.2014.03.022.
- 714 [40] T. Komatsu, H. Kawaide, C. Saito, A. Yamagami, S. Shimada, M. Nakazawa, M.
715 Matsui, A. Nakano, M. Tsujimoto, M. Natsume, H. Abe, T. Asami, T. Nakano, The
716 chloroplast protein BPG2 functions in brassinosteroid-mediated post-transcriptional
717 accumulation of chloroplast rRNA., *Plant J.* 61 (2010) 409–422. doi:10.1111/j.1365-
718 313X.2009.04077.x.
- 719 [41] R.M. Rivero, J. Gimeno, A. Van Deynze, H. Walia, E. Blumwald, Enhanced cytokinin
720 synthesis in tobacco plants expressing PSARK::IPT prevents the degradation of
721 photosynthetic protein complexes during drought, *Plant Cell Physiol.* 51 (2010)
722 1929–1941. doi:10.1093/pcp/pcq143.
- 723 [42] A. Harb, A. Krishnan, M.M.R. Ambavaram, A. Pereira, Molecular and physiological
724 analysis of drought stress in *Arabidopsis* reveals early responses leading to
725 acclimation in plant growth, *Plant Physiol.* 154 (2010) 1254–1271.
726 doi:10.1104/pp.110.161752.
- 727 [43] L. Li, C. Li, G.I. Lee, G. A. Howe, Distinct roles for jasmonate synthesis and action in
728 the systemic wound response of tomato, *Proc. Natl. Acad. Sci. U. S. A.* 99 (2002)
729 6416–6421. doi:10.1073/pnas.072072599.

- 730 [44] D.X. Xie, B.F. Feys, S. James, M. Nieto-Rostro, J.G. Turner, COI1: an Arabidopsis
731 gene required for jasmonate-regulated defense and fertility, *Science* 280 (1998)
732 1091–1094.
- 733 [45] J. Sun, V. Cardoza, D.M. Mitchell, L. Bright, G. Oldroyd, J.M. Harris, Crosstalk
734 between jasmonic acid, ethylene and Nod factor signaling allows integration of
735 diverse inputs for regulation of nodulation, *Plant J.* 46 (2006) 961–970.
736 doi:10.1111/j.1365-313X.2006.02751.x.
- 737 [46] C. Ellis, I. Karafyllidis, C. Wasternack, J.G. Turner, The Arabidopsis mutant *cev1*
738 links cell wall signaling to jasmonate and ethylene responses, *Plant Cell* 14 (2002)
739 1557–1566.
- 740 [47] N. Onkokesung, I. Gális, C.C. von Dahl, K. Matsuoka, H.-P. Saluz, I.T. Baldwin,
741 Jasmonic acid and ethylene modulate local responses to wounding and simulated
742 herbivory in *Nicotiana attenuata* leaves, *Plant Physiol.* 153 (2010) 785–798.
743 doi:10.1104/pp.110.156232.
- 744 [48] M.A. Bacon, The biochemical control of leaf expansion during drought. 101–112
745 *Plant Growth Regul.* 29 (1999) 101–112.
- 746 [49] D.J. Cosgrove, Expansive growth of plant cell walls, *Plant Physiol. Biochem.* 38
747 (2000) 109–124.
- 748 [50] D.J. Cosgrove, Loosening of plant cell walls by expansins, *Nature.* 407 (2000) 321–
749 326. doi:10.1038/35030000.
- 750 [51] K. Swarup, E. Benková, R. Swarup, I. Casimiro, B. Péret, Y. Yang, G. Parry, E.
751 Nielsen, I. De Smet, S. Vanneste, M.P. Levesque, D. Carrier, N. James, V. Calvo, K.
752 Ljung, E. Kramer, R. Roberts, N. Graham, S. Marillonnet, K. Patel, J.D.G. Jones,
753 C.G. Taylor, D.P. Schachtman, S. May, G. Sandberg, P. Benfey, J. Friml, I. Kerr, T.
754 Beeckman, L. Laplaze, M.J. Bennett, The auxin influx carrier LAX3 promotes lateral
755 root emergence, *Nat. Cell Biol.* 10 (2008) 946–954. doi:10.1038/ncb1754.

- 756 [52] D. Todaka, K. Shinozaki, K. Yamaguchi-Shinozaki, Recent advances in the
757 dissection of drought-stress regulatory networks and strategies for development of
758 drought-tolerant transgenic rice plants, *Front. Plant Sci.* 6 (2015) 84.
759 doi:10.3389/fpls.2015.00084.
- 760 [53] R. Tanaka, A. Tanaka, Tetrapyrrole Biosynthesis in Higher Plants, *Annu. Rev. Plant*
761 *Biol.* 58 (2007) 321–46. doi:10.1146/annurev.arplant.57.032905.105448.
- 762 [54] Y.B. Yun, J.I. Park, H.S. Choi, H. Jung, S.J. Jang, K. Back, Y.I. Kuk,
763 Protoporphyrinogen oxidase-overexpressing transgenic rice is resistant to drought
764 stress, *Crop Sci.* 53 (2013) 1076–1085.
- 765 [55] T.H. Phung, H. Jung, J.H. Park, J.G. Kim, K. Back, S. Jung, Porphyrin biosynthesis
766 control under water stress: Sustained porphyrin status correlates with drought
767 tolerance in transgenic rice, *Plant Physiol.* 157 (2011) 1746–1764.
768 doi:10.1104/pp.111.188276.
- 769 [56] D.S.K. Nagahatenna, P. Langridge, R. Whitford, Tetrapyrrole-based drought stress
770 signalling, *Plant Biotechnol. J.* 13 (2015) 447–459. doi:10.1111/pbi.12356.
- 771 [57] M. Gabruk, B. Mysliwa-Kurdziel, Light-Dependent Protochlorophyllide
772 Oxidoreductase: Phylogeny, Regulation, and Catalytic Properties, *Biochemistry.* 54
773 (2015) 5255–5262. doi:10.1021/acs.biochem.5b00704.
- 774 [58] R.D. Willows, Biosynthesis of chlorophylls from protoporphyrin IX, *Nat. Prod. Rep.* 20
775 (2015) 327-341
- 776 [59] G.H. Krause, movement of magnesium ions in intact chloroplasts, Spectroscopic
777 determination with Eriochrome Blue SE, *BBA-Bioenergetics* 460 (1977) 500–510.
- 778 [60] W.H. Heldt, K. Werdan, M. Milovancev, G. Geller, Alkalization of the chloroplast
779 stroma caused by light-dependent proton flux into the thylakoid space, *Biochim.*
780 *Biophys. Acta.* 314 (1973) 224–241.

- 781 [61] K. Werdan, H.W. Heldt, M. Milovancev, The role of pH in the regulation of carbon
782 fixation in the chloroplast stroma. *Studies on CO₂ fixation in the light and dark*,
783 *Biochim. Biophys. Acta.* 396 (1975) 276–292.
- 784 [62] W.L. Araújo, A.O. Martins, A.R. Fernie, T. Tohge, 2-Oxoglutarate: linking TCA cycle
785 function with amino acid, glucosinolate, flavonoid, alkaloid, and gibberellin
786 biosynthesis, *Front. Plant Sci.* 5 (2014) 552. doi:10.3389/fpls.2014.00552.
- 787 [63] M. Hodges, Enzyme redundancy and the importance of 2-oxoglutarate in plant
788 ammonium assimilation, *J. Exp. Bot.* 53 (2002) 905–916.
- 789 [64] A. Strand, T. Asami, J. Alonso, J.R. Ecker, J. Chory, Chloroplast to nucleus
790 communication triggered by accumulation of Mg-protoporphyrinIX, *Nature.* 421
791 (2003) 79–83. doi:10.1038/nature01204.
- 792 [65] Y. Kanesaki, Y. Kobayashi, M. Hanaoka, K. Tanaka, Mg-protoporphyrin IX signaling
793 in *Cyanidioschyzon merolae*: multiple pathways may involve the retrograde signaling
794 in plant cells, *Plant Signal. Behav.* 4 (2009) 1190–1192.
- 795 [66] L.B. Davin, N.G. Lewis, Dirigent proteins and dirigent sites explain the mystery of
796 specificity of radical precursor coupling in lignan and lignin biosynthesis, *Plant*
797 *Physiol.* 123 (2000) 453–462.
- 798 [67] S. Subramanyam, C. Zheng, J.T. Shukle, , CE, Williams, Hessian fly larval attack
799 triggers elevated expression of disease resistance dirigent-like protein-encoding
800 gene, *HfrDrd*, in resistant wheat, *Arthropod Plant Interact.* 7 (2013) 389–402.
- 801 [68] X. Liu, J. Bai, L. Huang, L. Zhu, X. Liu, N. Weng, J.C. Reese, M. Harris, J.J. Stuart,
802 M.-S. Chen, Gene expression of different wheat genotypes during attack by virulent
803 and avirulent hessian fly (*Mayetiola destructor*) Larvae, *J. Chem. Ecol.* 33 (2007)
804 2171–2194. doi:10.1007/s10886-007-9382-2.
- 805 [69] D.K. Kosma, J.A. Nemacheck, M.A. Jenks, C.E. Williams, Changes in properties of
806 wheat leaf cuticle during interactions with Hessian fly, *Plant J.* 63 (2010) 31–43.
807 doi:10.1111/j.1365-313X.2010.04229.x.

- 808 [70] K. Vissenberg, M. Oyama, Y. Osato, R. Yokoyama, J.-P. Verbelen, K. Nishitani,
809 Differential expression of AtXTH17, AtXTH18, AtXTH19 and AtXTH20 genes in
810 Arabidopsis roots. Physiological roles in specification in cell wall construction, *Plant*
811 *Cell Physiol.* 46 (2005) 192–200. doi:10.1093/pcp/pci013.
- 812 [71] D. J. Cosgrove, Plant cell wall extensibility: connecting plant cell growth with cell wall
813 structure, mechanics, and the action of wall-modifying enzymes, *J. Exp. Bot.* 67
814 (2015) 463–476.
- 815 [72] G. Li, V. Santoni, C. Maurel, Plant aquaporins: Roles in plant physiology, *Biochim.*
816 *Biophys. Acta - Gen. Subj.* 1840 (2014) 1574–1582.
817 doi:10.1016/j.bbagen.2013.11.004.
- 818 [73] W.A. Snedden, H. Fromm, Calmodulin, calmodulin-related proteins and plant
819 responses to the environment, *Trends Plant Sci.* 3 (2016) 299–304.
820 doi:10.1016/S1360-1385(98)01284-9.
- 821 [74] R.E. Zielinski, Calmodulin and calmodulin-binding proteins in plants, *Annu. Rev.*
822 *Plant Physiol. Plant Mol. Biol.* 49 (1998) 697–725.
- 823 [75] N. Pandey, A. Ranjan, P. Pant, R. Tripathi, F. Ateek, H. Pandey, U. Patre, S. Sawant,
824 CAMTA 1 regulates drought responses in *Arabidopsis thaliana*, *BMC Genomics.* 14
825 (2013) 216. doi:10.1186/1471-2164-14-216.
- 826 [76] Z. Wang, W. Xie, F. Chi, C. Li, Identification of non-specific lipid transfer protein-1 as
827 a calmodulin-binding protein in *Arabidopsis*, *FEBS Lett.* 579 (2005) 1683–1687.
828 doi:10.1016/j.febslet.2005.02.024.
- 829 [77] F. Bourgis, J.-C. Kader, Lipid-transfer proteins: Tools for manipulating membrane
830 lipids, *Physiol. Plant.* 100 (1997) 78–84. doi:10.1111/j.1399-3054.1997.tb03456.x.
- 831 [78] P. Sterk, H. Booij, G.A. Schellekens, A. Van Kammen, S.C. De Vries, Cell-specific
832 expression of the carrot EP2 lipid transfer protein gene, *Plant Cell.* 3 (1991) 907–921.
833 doi:10.1105/tpc.3.9.907.

- 834 [79] K.R. Kottapalli, R. Rakwal, J. Shibato, G. Burow, D. Tissue, J. Burke, N. Puppala, M.
835 Burow, P. Payton, Physiology and proteomics of the water-deficit stress response in
836 three contrasting peanut genotypes, *Plant. Cell Environ.* 32 (2009) 380–407.
837 doi:10.1111/j.1365-3040.2009.01933.x.
- 838 [80] A.A. Rodríguez-Hernández, M.A. Ortega-Amaro, P. Delgado-Sánchez, J. Salinas,
839 J.F. Jiménez-Bremont, AtGRDP1 gene encoding a glycine-rich domain protein is
840 involved in germination and responds to aba signalling, *Plant Mol. Biol. Rep.* 32
841 (2014) 1187–1202
- 842 [81] R. Long, Q. Yang, J. Kang, T. Zhang, H. Wang, M. Li, Z. Zhang, Overexpression of a
843 novel salt stress-induced glycine-rich protein gene from alfalfa causes salt and ABA
844 sensitivity in *Arabidopsis*, *Plant Cell Rep.* 32 (2013) 1289–1298. doi:10.1007/s00299-
845 013-1443-0.
- 846 [82] C. Urbez, M. Cercós, M.A. Perez-Amador, J. Carbonell, Expression of PsGRP1, a
847 novel glycine rich protein gene of *Pisum sativum*, is induced in developing fruit and
848 seed and by ABA in pistil and root, *Planta.* 223 (2006) 1292–1302.
849 doi:10.1007/s00425-005-0178-8.
- 850 [83] A.S. Reddy, B.W. Poovaiah, Accumulation of a glycine rich protein in auxin-deprived
851 strawberry fruits, *Biochem. Biophys. Res. Commun.* 147 (1987) 885–891.
- 852 [84] J.A. Huerta-Ocampo, M.F. León-Galván, L.B. Ortega-Cruz, A. Barrera-Pacheco, A.
853 De León-Rodríguez, G. Mendoza-Hernández, A.P.B. de la Rosa, Water stress
854 induces up-regulation of DOF1 and MIF1 transcription factors and down-regulation of
855 proteins involved in secondary metabolism in amaranth roots (*Amaranthus*
856 *hypochondriacus* L.), *Plant Biol. (Stuttg).* 13 (2011) 472–482. doi:10.1111/j.1438-
857 8677.2010.00391.x.
- 858
- 859

860 **TABLES**

861 **Table 1.** Biomass of wheat plants grown from sedaxane treated and untreated seeds 36
862 days after germination. Each value is a mean (n=7) followed by standard error. SDX,
863 sedaxane. UNT, untreated. AW_{FC} , available water at field capacity

864 **Table 2.** Mapman functional categories (BINs) in the cell function pathway for significantly
865 up-and down-regulated genes (≥ 1.5 -fold change; $P < 0.05$) in (A) seeds after 48 h
866 pregermination, and in (B) roots and (C) leaves of wheat plants grown from sedaxane
867 treated and untreated seeds under drought stress (10% AW_{FC}) 9 days after germination.

868 **Table 3.** Mapman functional categories in the metabolic pathways for significantly up-and
869 down-regulated genes (≥ 1.5) in leaves of wheat plants grown from sedaxane treated and
870 untreated seeds under drought stress (10% AW_{FC}) 9 days after germination.

871 **Table 4.** GO enrichment analysis for significantly up-and down-regulated genes (≥ 1.5 -fold
872 change; $P < 0.05$) in seeds after 48 h pregermination. Analysis was performed using
873 parametric analysis of gene set enrichment in AgriGO with Bonferroni multitest adjustment
874 method. FC, fold change; FDR, false discovery rate; P, biological process; F, molecular
875 function; C, cellular component. Red color system indicates upregulated and blue indicate
876 downregulated terms.

877 **Table 5.** GO enrichment analysis for significantly up-and down-regulated genes (≥ 1.5 -fold
878 change; $P < 0.05$) in leaves of wheat plants grown from sedaxane treated and untreated
879 seeds under drought stress (10% AW_{FC}) 9 days after germination. Analysis was performed
880 using analysis of gene set enrichment in AgriGO with Bonferroni multitest adjustment
881 method. FC, fold change; FDR, false discovery rate; P, biological process; F, molecular
882 function; C, cellular component. Red color system indicates upregulated and blue indicate
883 downregulated terms.

884 **FIGURES**

885 **Fig. 1.** A, Efficiency of photosystem II (PSII) photochemistry (F_v'/F_m') in light adapted
886 samples; B, Quantum yield (QY); C, Dissipated energy flux per active reaction center
887 (D_{lo}/RC), of leaves of wheat seedlings grown from sedaxane treated and untreated seeds.
888 Error bars indicate mean \pm SE, $n = 7$. Asterisks indicate significant difference ($P < 0.05$) from
889 the untreated control. SDX, Sedaxane, UNT, Untreated.

890 **Fig. 2.** Light response of photochemical quenching (qP) of drought-stressed (10% AW_{FC})
891 and non-stressed (90% AW_{FC}) plants 12 days after germination. Error bars indicate mean \pm
892 SE, $n = 7$. Asterisks show a significant difference ($P < 0.05$) from the untreated control. AW_{FC}
893 - available water at field capacity.

894 **Fig. 3.** Light response of A, dissipated excess excitation energy measured as non-
895 photochemical quenching (NPQ) and B, rate of CO_2 assimilation (A) in leaves of wheat
896 plants grown from sedaxane treated and untreated seeds 12 DAG. Error bars indicate mean
897 \pm SE, $n = 7$. Asterisks in A, indicate differences ($P < 0.05$) from the untreated control. In B,
898 asterisks indicate significant interaction ($P < 0.05$) between fungicide sedaxane and available
899 water at field capacity (AW_{FC}). SDX, sedaxane. UNT, Untreated.

900 **Fig. 4.** Venn diagram comparing up-regulated genes (adjusted $P < 0.05$; Fold change ≥ 1.5)
901 in leaf and root tissues of plants grown from sedaxane treated seeds and treated seed after
902 48hr pregermination.

903 **Fig. 5.** Coexpression and regulatory interaction network of common top differentially
904 expressed genes across the tissues (leaf, root and pregerminated seeds). The subnetwork
905 was implemented and visualized in Cytoscape. Nodes were coloured based on stress
906 degree, red, brown and yellow represented highest, high and middle stress respectively. The
907 edge colour and thickness represent the degree of co-expressed connections from strong
908 (thick and brown) to weak (thin and green).

909 **Fig. 6.** Expression levels of candidate genes by microarray and qRT-PCR. Genes were
910 selected from gene network analysis across leaf, root and pregerminated tissues. The array
911 and qRT-PCR data are averages of 3 biological replicates of minimum of 3 plants each.
912 Error bars indicate mean \pm SE. Asterisks show significant differences in candidate gene
913 expression levels compared to the corresponding control (* $P < 0.05$). NE: new experiment.

914 **Fig. 7.** Molecular responses to sedaxane in individual plant tissues and across tissues and
915 their effect on plant physiology. Sedaxane induced transcriptional regulation of genes and
916 transcriptional factors resulting in protection against oxidative stress in pregerminated seeds,
917 downregulation of pathogenesis related genes at 9 days after germination under drought
918 conditions in the root tissues; coupled with altered hormone signaling and metabolism in the
919 leaves to mobilize metabolites towards growth and adaptive development leading to
920 increased drought tolerance with improved photosynthesis and growth.

921

922 **Appendix A. Supplementary data**

923 **Fig. S1.** Light response of plants drought-stressed (10% AW_{FC}) and non-stressed (90%
924 AW_{FC}) plants 12 days after germination. A, Stomatal conductance. B, Transpiration rates.
925 Error bars indicate mean \pm SE, n = 7. Asterisks show a significant difference ($P < 0.05$) from
926 the untreated control. AW_{FC} - available water at field capacity.

927 **Table S1.** List of targeted genes for qRT-PCR.

928 **Table S4.** Functional categories in the MapMan 'metabolism overview' of differentially
929 regulated genes (adjusted $P < 0.05$) in the leaf of drought stressed wheat plants grown from
930 sedaxane treated seeds.

931 **Table S5.** Centralities based analysis and the values of the top 40 ranked genes

932 **Appendix B. Supplementary data**

933 **Table S2.**

934 **A.** Differentially regulated transcripts (adjusted $P < 0.05$) in sedaxane treated- pregerminated
935 seeds

936 **B.** Differentially regulated transcripts (adjusted $P < 0.05$) in the root of drought stressed wheat
937 plants grown from sedaxane treated seeds

938 **C.** Differentially regulated transcripts (adjusted $P < 0.05$) in the leaf of drought stressed wheat
939 plants grown from sedaxane treated seeds

940 **Appendix C. Supplementary data**

941 **Table S3.**

942 **A.** Functional categories in the Mapman 'cell function overview' of differentially regulated
943 genes (adjusted $P < 0.05$) in sedaxane treated pregerminated seeds

944 **B.** Functional categories in the MapMan 'cell function overview' of differentially regulated
945 genes (adjusted $P < 0.05$) in the root of drought stressed wheat plants grown from sedaxane
946 treated seeds.

947 **C.** Functional categories in the MapMan 'cell function overview' of differentially regulated
948 genes (adjusted $P < 0.05$) in the leaf of drought stressed wheat plants grown from sedaxane
949 treated seeds.

950

951

1 **TABLE 1.**

2 Biomass of wheat plants grown from sedaxane treated and untreated seeds 36 days after germination.

Fungicide	Tiller no.		Height (cm)		Water content (%)		Dry weight (g)	
	10% AW _{FC}	90% AW _{FC}	10% AW _{FC}	90% AW _{FC}	10% AW _{FC}	90% AW _{FC}	10% AW _{FC}	90% AW _{FC}
SDX	8 ± 1	35 ± 2	18.31 ± 0.23	36.05 ± 0.48	73.51 ± 2.77	86.68 ± 0.51	0.27 ± 0.03	0.13 ± 0.01
UNT	7 ± 1	33 ± 2	17.03 ± 0.51	36.71 ± 0.52	83.12 ± 1.1	88.4 ± 0.95	0.17 ± 0.01	0.12 ± 0.01
Effects	P	LSD	P	LSD	P	LSD	P	LSD
Fungicide	0.432	3.176	0.478	0.955	0.003	3.438	0.003	0.035
AW _{FC}	<0.001	3.176	<0.001	0.955	<0.001	3.438	<0.001	0.035
Fungicide x AW _{FC}	0.547	4.491	0.044	1.351	0.027	4.862	0.027	0.049

3 Each value is a mean (n=7) followed by standard error. SDX, sedaxane. UNT, untreated. AW_{FC}, available water at field capacity. Dry weight is
4 expressed relative to fresh weight

5

1 **TABLE 2.**

2 Mapman functional categories (BINs) in the cell function pathway for significantly up-and
 3 down-regulated genes (≥ 1.5 fold change; $P < 0.05$) in (A) seeds after 48 hrs pregermination,
 4 and in (B) roots and (C) leaves of wheat plants grown from sedaxane treated and untreated
 5 seeds under drought stress (10% AW_{FC}) 9 days after germination.

	Bin	Name	Up	Down	P Value
A. Pregerminated seeds	28.1	DNA.synthesis/Chromatin structure.histone	2	84	3.67E-12
	20.1	Stress.biotic	3	18	2.30E-02
	35.2	Not assigned/unknown	355	750	1.10E-02
B. Roots	20.1	Stress. biotic	0	10	2.00E-02
C. Leaves	29.2	Protein synthesis	58	16	6.56E-13
	17	Hormone metabolism	5	47	2.20E-07
	20.1	Stress.biotic	4	29	3.84E-05
	29.4	Protein.postranslational	7	35	5.40E-02
	30	Signalling	13	53	5.40E-02
	26	Misc	65	54	5.40E-02

6 AW_{FC} , available water at field capacity

7

1 **TABLE 3.**

2 Mapman functional categories in the metabolic pathway for significantly up-and down-
3 regulated genes (≥ 1.5) in leaves of wheat plants grown from sedaxane treated and
4 untreated seeds under drought stress (10% AW_{FC}) 9 days after germination.

Bin	Name	Up	Down	<i>P</i> value
10.7	Cell wall.modification	12	1	2.64E-06
19	Tetrapyrrole synthesis	8	0	4.00E-02

5 AW_{FC} , available water at field capacity

6

1 **TABLE 4.**

2 GO enrichment analysis of pathways for significantly up-and down-regulated genes (≥ 1.5
3 fold change; $P < 0.05$) in seeds after 48 h pregermination.

GO Term	Ontology Source	Description	No. Input List	Mean Log ₂ FC	Z-score	FDR
GO:0006575	P	cellular amino acid derivative metabolic process	20	0.28	3.3	8.70E-03
GO:0006790	P	sulfur metabolic process	16	0.37	3.3	8.70E-03
GO:0006803	P	glutathione conjugation reaction	10	0.59	3.3	8.70E-03
GO:0006749	P	glutathione metabolic process	10	0.59	3.3	8.70E-03
GO:0006518	P	peptide metabolic process	10	0.59	3.3	8.70E-03
GO:0051186	P	cofactor metabolic process	18	0.26	3.1	1.40E-02
GO:0009057	P	macromolecule catabolic process	13	0.36	3	2.00E-02
GO:0006732	P	coenzyme metabolic process	15	0.27	2.8	2.80E-02
GO:0006091	P	generation of precursor metabolites and energy	19	0.17	2.8	3.30E-02
GO:0009056	P	catabolic process	22	0.09	2.6	4.70E-02
GO:0051707	P	response to other organism	18	-1.2	-2.6	4.70E-02
GO:0009607	P	response to biotic stimulus	23	-1.1	-2.7	4.60E-02
GO:0044085	P	cellular component biogenesis	40	-1	-3.1	1.40E-02
GO:0065003	P	macromolecular complex assembly	35	-1.1	-3.3	8.70E-03
GO:0043933	P	macromolecular complex subunit organization	35	-1.1	-3.3	8.70E-03
GO:0034622	P	cellular macromolecular complex assembly	35	-1.1	-3.3	8.70E-03
GO:0034621	P	cellular macromolecular complex subunit organization	35	-1.1	-3.3	8.70E-03
GO:0022607	P	cellular component assembly	35	-1.1	-3.3	8.70E-03
GO:0016043	P	cellular component organization	50	-1	-3.5	6.90E-03
GO:0051276	P	chromosome organization	36	-1.2	-3.7	3.90E-03
GO:0006996	P	organelle organization	42	-1.1	-3.7	3.90E-03
GO:0065004	P	protein-DNA complex assembly	29	-1.3	-3.8	2.90E-03
GO:0034728	P	nucleosome organization	29	-1.3	-3.8	2.90E-03
GO:0031497	P	chromatin assembly	29	-1.3	-3.8	2.90E-03
GO:0006334	P	nucleosome assembly	29	-1.3	-3.8	2.90E-03
GO:0006323	P	DNA packaging	30	-1.2	-3.8	2.90E-03
GO:0006333	P	chromatin assembly or disassembly	31	-1.3	-4	2.90E-03
GO:0006325	P	chromatin organization	33	-1.2	-4	2.90E-03
GO:0071103	P	DNA conformation change	31	-1.3	-4	2.90E-03
GO:0004364	F	glutathione transferase activity	12	0.74	4.1	4.20E-03
GO:0048037	F	cofactor binding	32	0.15	3.5	1.30E-02
GO:0016765	F	transferase activity, transferring alkyl or aryl (other than methyl) groups	14	0.46	3.4	1.40E-02
GO:0003676	F	nucleic acid binding	96	-0.85	-3.2	2.50E-02
GO:0003677	F	DNA binding	79	-0.93	-3.5	1.30E-02

4 Analysis was performed using parametric analysis of gene set enrichment in AgriGO with
5 Bonferroni multitest adjustment method. FC, fold change; FDR, false discovery rate; P,
6 biological process; F, molecular function; C, cellular component. Red color system indicates
7 upregulated and blue indicate downregulated terms

1 **TABLE 5.**

2 GO enrichment analysis of pathways for significantly up-and down-regulated genes (≥ 1.5 fold change; $P < 0.05$) in
 3 leaves of wheat plants grown from sedaxane treated and untreated seeds under drought stress (10% AW_{FC}) 9 days
 4 after germination.

GO Term	Ontology Source	Description	No. Input List	Mean \log_2FC	Z-score	FDR
GO:0006412	P	translation	56	0.56	6.3	5.10E-08
GO:0042254	P	ribosome biogenesis	41	0.59	5.6	2.00E-06
GO:0022613	P	ribonucleoprotein complex biogenesis	42	0.56	5.5	3.10E-06
GO:0044085	P	cellular component biogenesis	57	0.34	4.5	2.00E-04
GO:0009059	P	macromolecule biosynthetic process	123	0.15	4.1	9.30E-04
GO:0034645	P	cellular macromolecule biosynthetic process	109	0.12	3.5	8.50E-03
GO:0044249	P	cellular biosynthetic process	208	0.04	3.4	8.50E-03
GO:0033013	P	tetrapyrrole metabolic process	11	0.72	3.4	8.50E-03
GO:0015994	P	chlorophyll metabolic process	11	0.72	3.4	8.50E-03
GO:0006778	P	porphyrin metabolic process	11	0.72	3.4	8.50E-03
GO:0009058	P	biosynthetic process	220	0.03	3.4	9.60E-03
GO:0010467	P	gene expression	108	0.09	3.1	2.50E-02
GO:0009309	P	amine biosynthetic process	11	0.58	2.9	3.90E-02
GO:0008652	P	cellular amino acid biosynthetic process	11	0.58	2.9	3.90E-02
GO:0044267	P	cellular protein metabolic process	146	0.03	2.8	4.60E-02
GO:0009607	P	response to biotic stimulus	26	-0.64	-2.8	4.60E-02
GO:0051707	P	response to other organism	24	-0.69	-3	3.30E-02
GO:0051704	P	multi-organism process	24	-0.69	-3	3.30E-02
GO:0006952	P	defense response	31	-0.74	-3.7	4.50E-03
GO:0009695	P	jasmonic acid biosynthetic process	11	-1.3	-4.5	2.00E-04
GO:0009694	P	jasmonic acid metabolic process	11	-1.3	-4.5	2.00E-04
GO:0031408	P	oxylipin biosynthetic process	20	-1	-4.5	2.00E-04
GO:0031407	P	oxylipin metabolic process	20	-1	-4.5	2.00E-04
GO:0003735	F	structural constituent of ribosome	61	0.57	6.7	1.40E-09
GO:0005198	F	structural molecule activity	66	0.54	6.7	1.40E-09
GO:0019843	F	rRNA binding	17	0.97	5.4	1.60E-06
GO:0003723	F	RNA binding	42	0.50	5	6.30E-06
GO:0016757	F	transferase activity, transferring glycosyl groups	32	0.32	3.2	1.20E-02
GO:0016758	F	transferase activity, transferring hexosyl groups	24	0.35	2.9	2.90E-02
GO:0032561	F	guanyl ribonucleotide binding	11	0.55	2.8	3.60E-02
GO:0019001	F	guanyl nucleotide binding	11	0.55	2.8	3.60E-02
GO:0005525	F	GTP binding	11	0.55	2.8	3.60E-02
GO:0048037	F	cofactor binding	32	-0.58	-2.7	4.40E-02
GO:0050662	F	coenzyme binding	25	-0.65	-2.8	3.60E-02
GO:0004674	F	protein serine/threonine kinase activity	44	-0.78	-4.7	2.40E-05
GO:0004672	F	protein kinase activity	58	-0.74	-5.1	5.70E-06
GO:0016772	F	transferase activity, transferring phosphorus-containing groups	97	-0.61	-5.1	5.70E-06
GO:0016773	F	phosphotransferase activity, alcohol group as acceptor	64	-0.74	-5.3	2.70E-06
GO:0016301	F	kinase activity	83	-0.67	-5.3	2.50E-06

5 Analysis was performed using analysis of gene set enrichment in AgriGO with Bonferroni multitest adjustment method.
 6 FC, fold change; FDR, false discovery rate; P, biological process; F, molecular function; C, cellular component. Red
 7 color system indicates upregulated and blue indicate downregulated terms. AW_{FC} , available water at field capacity

Fig. 1

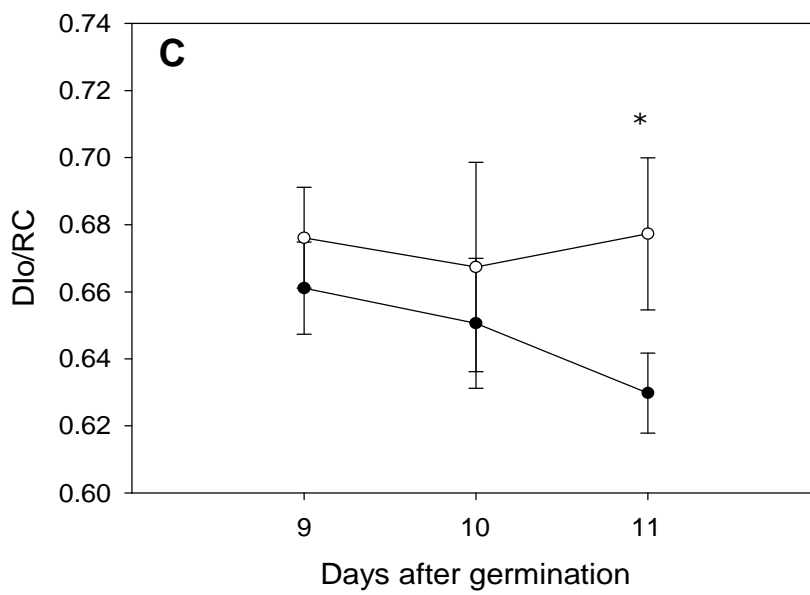
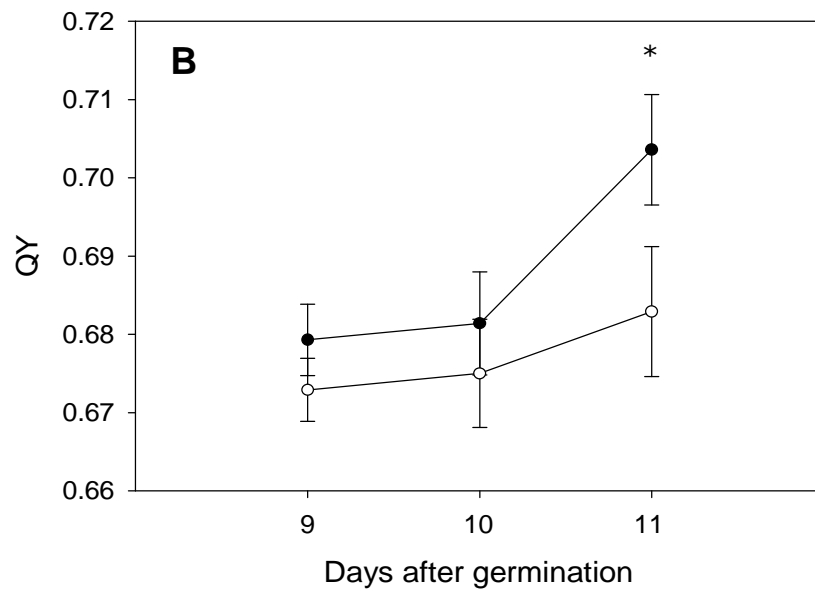
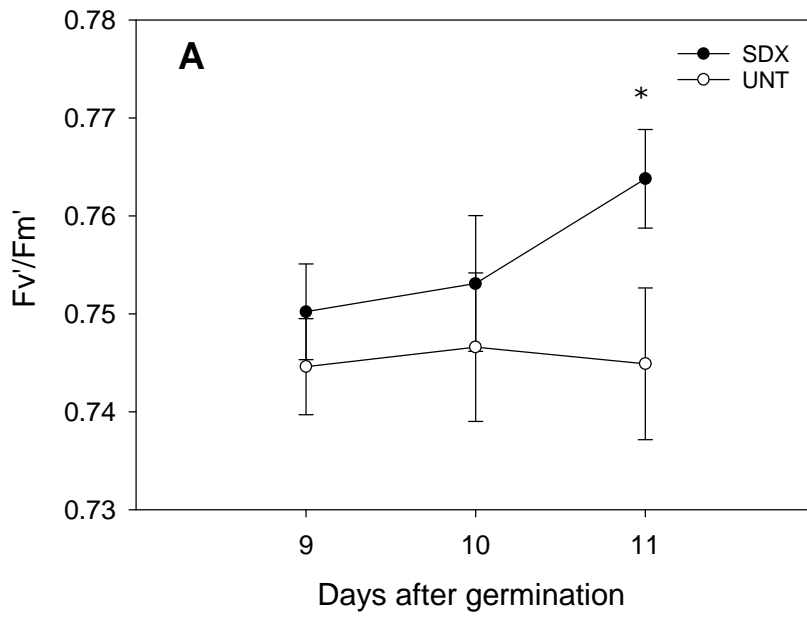


Fig. 2.

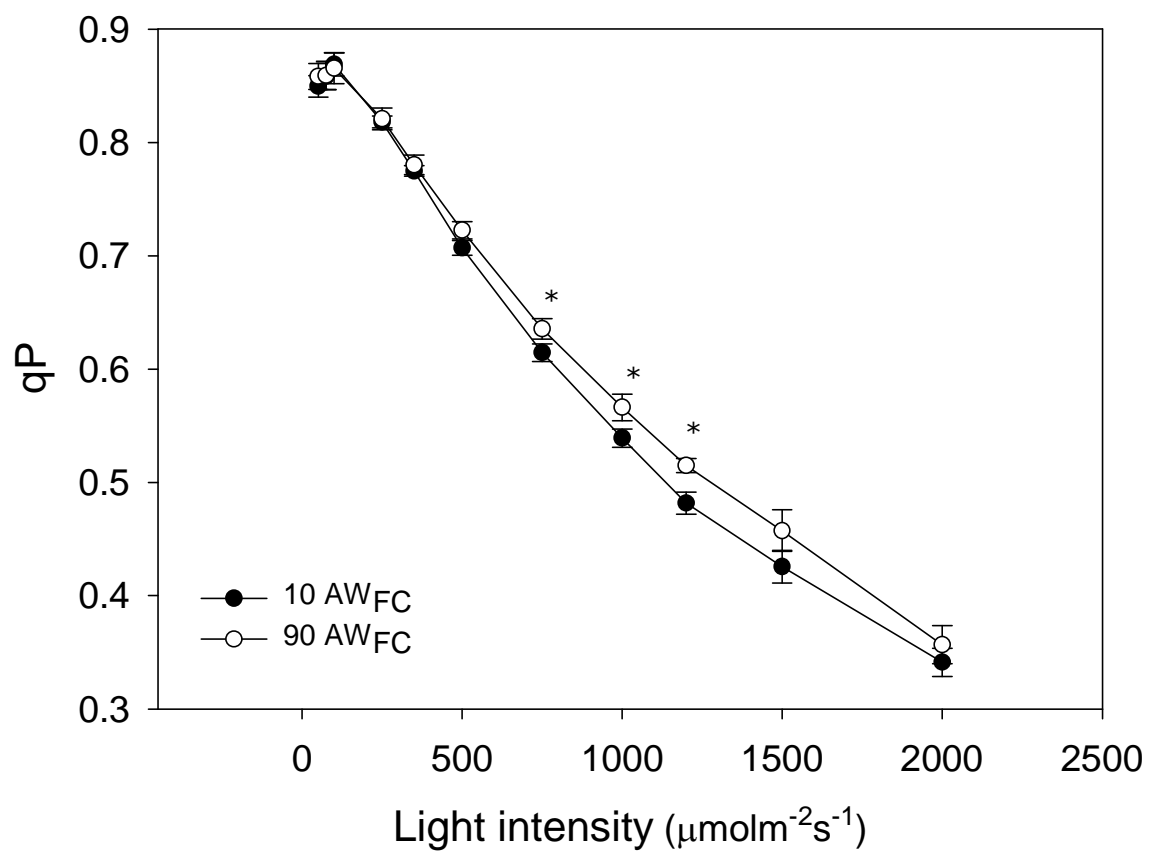


Fig. 3.

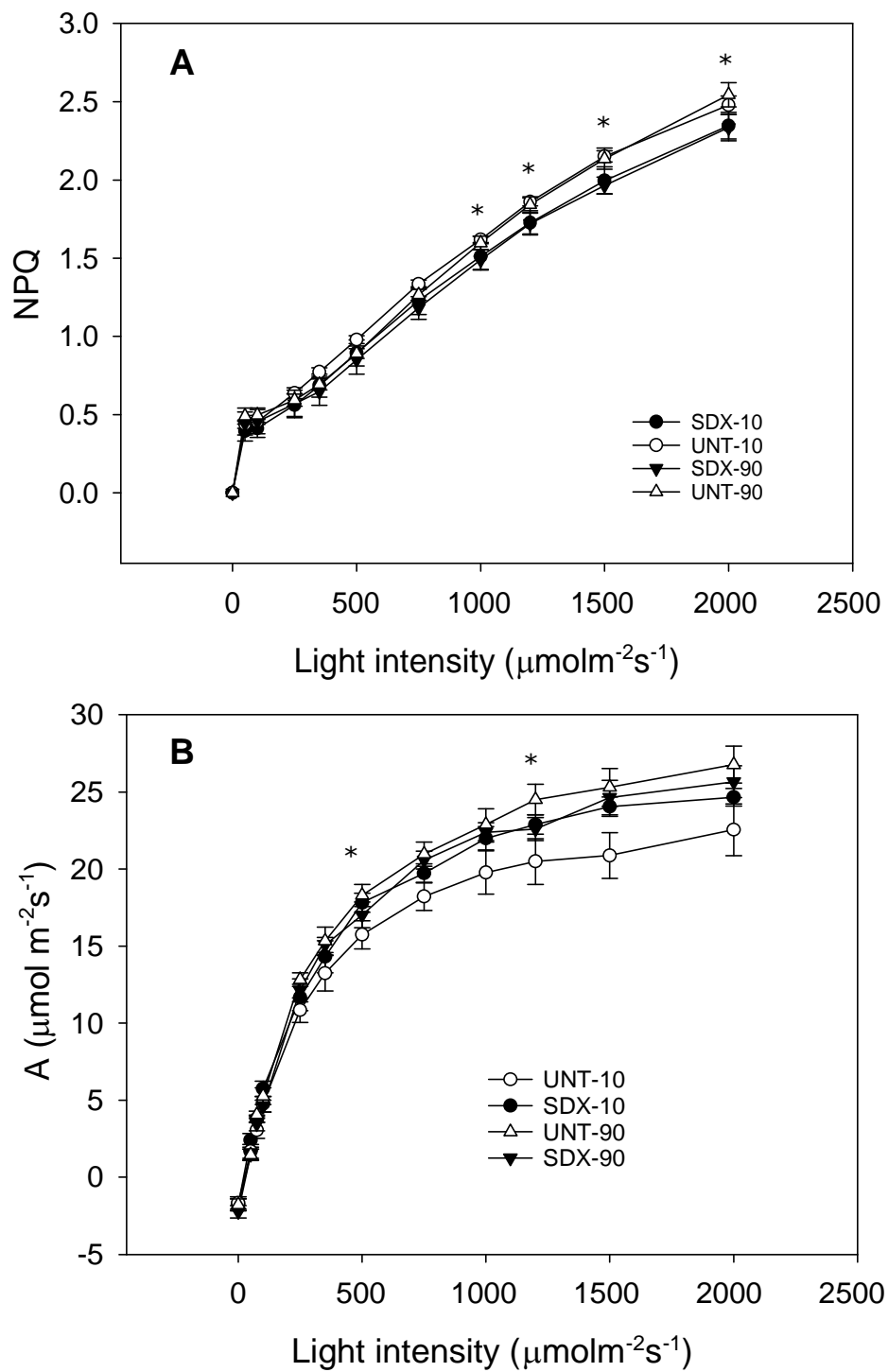


Fig. 4.

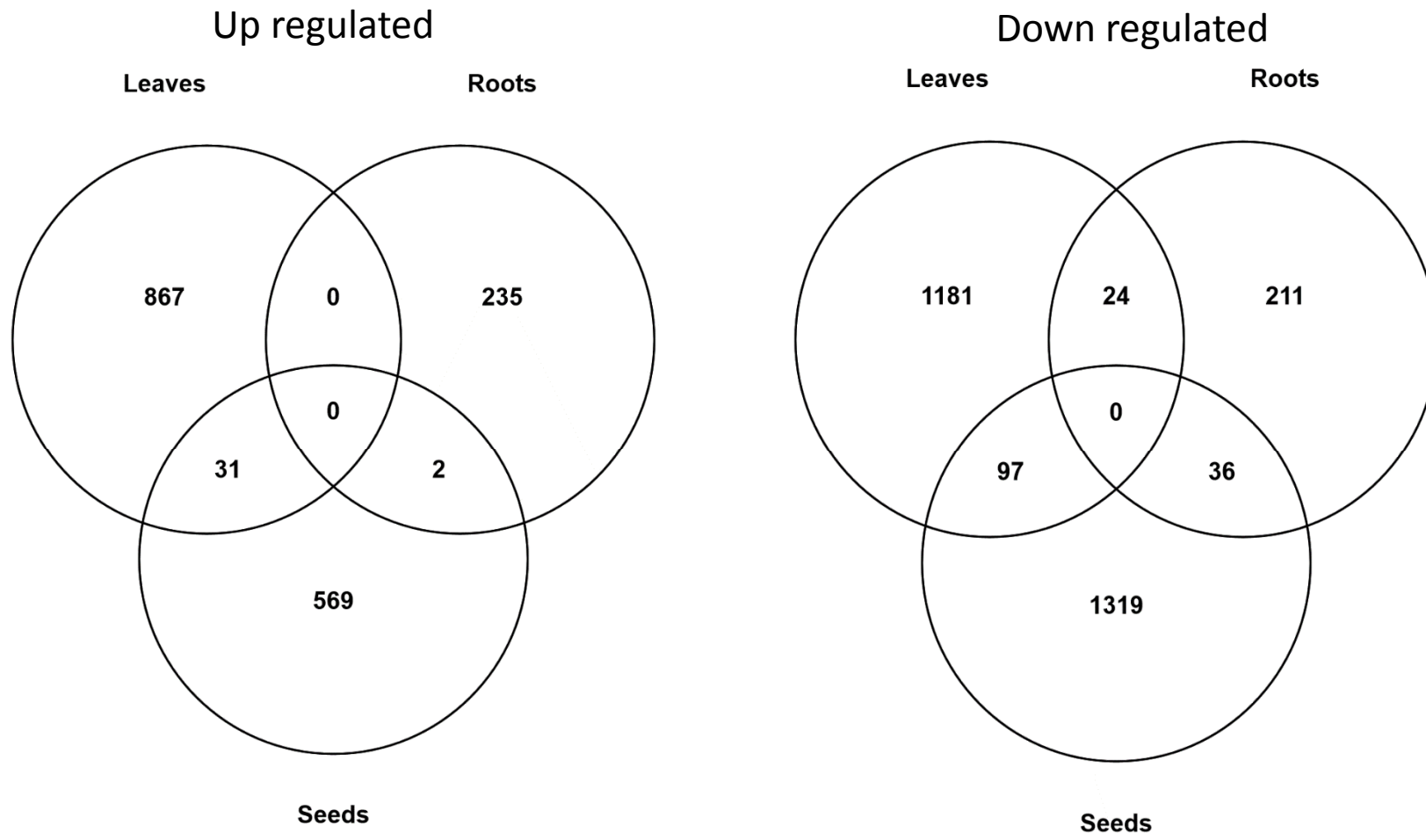


Fig. 5.

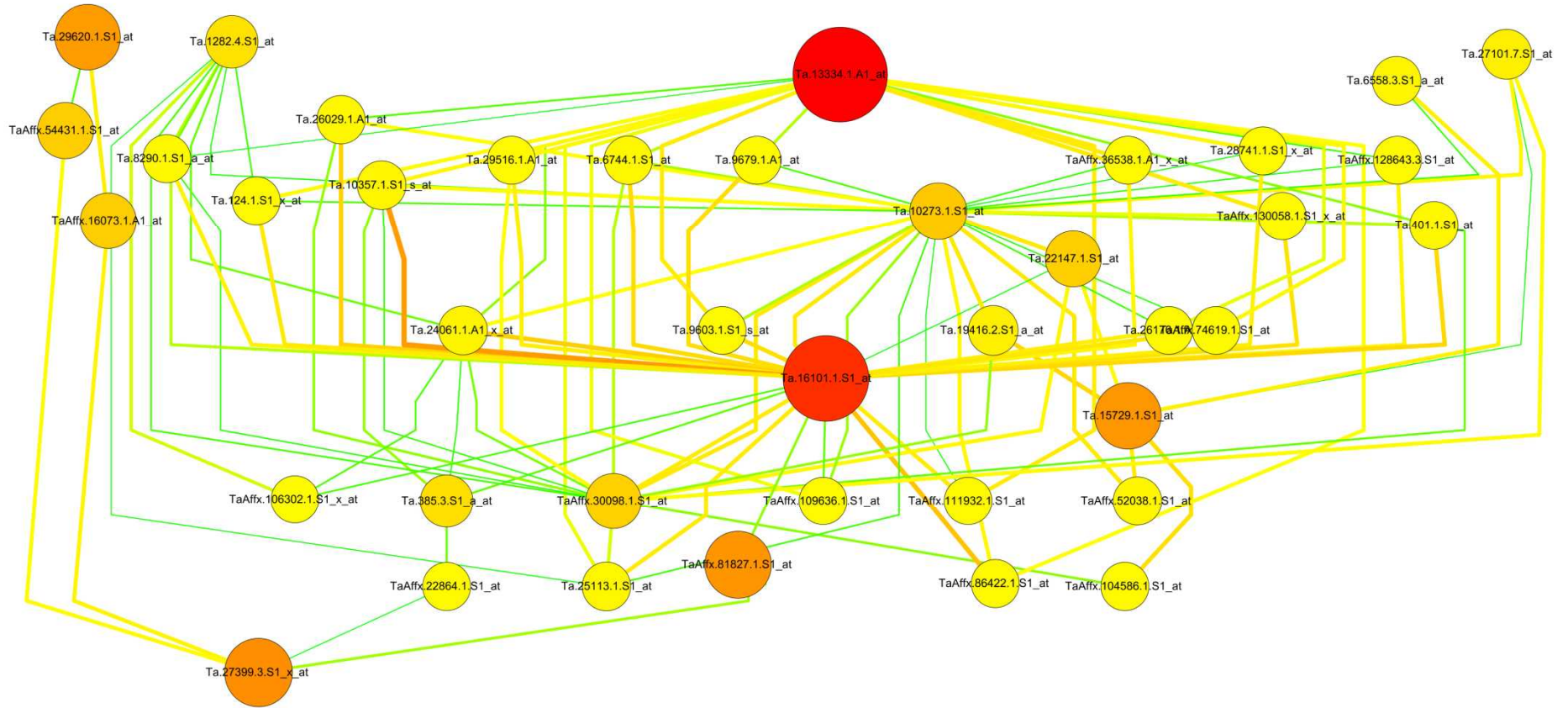


Fig. 6.

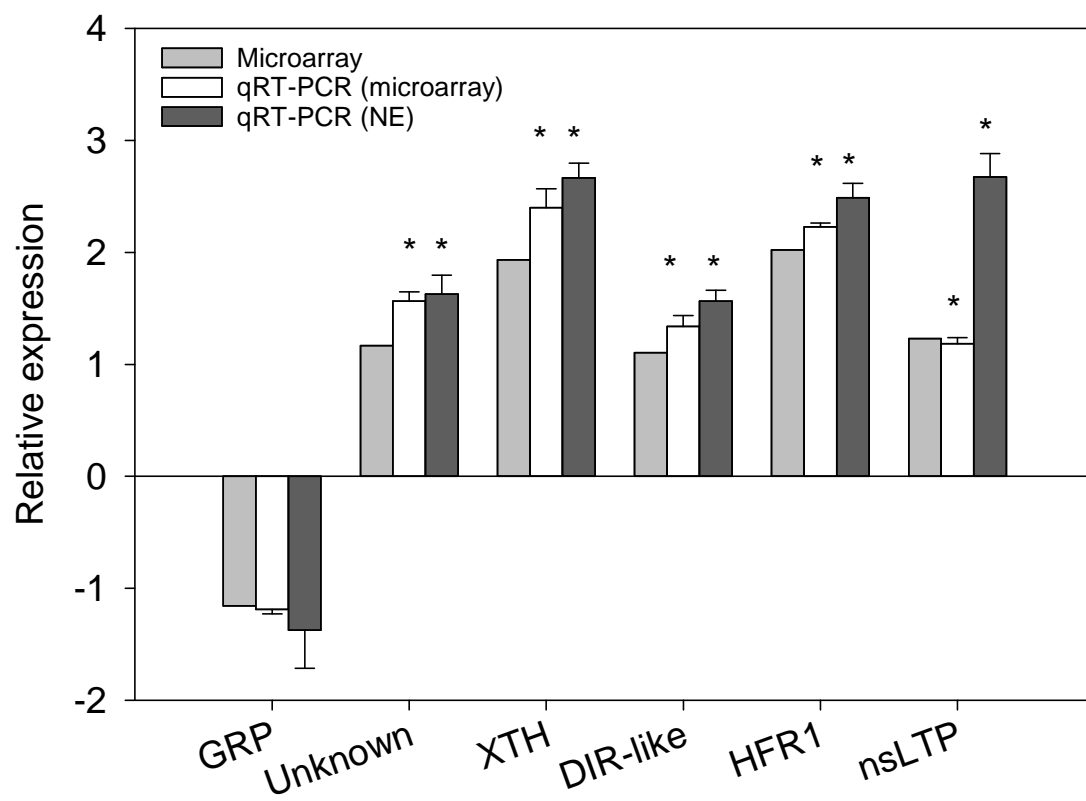


Fig. 7.

